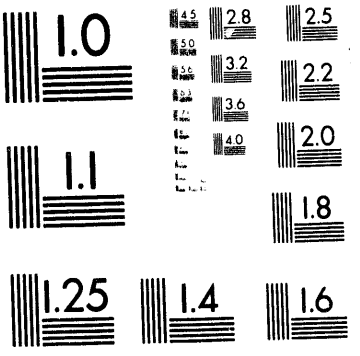
1.0
4.5
2.8
2.5
5.0
3.2
2.2
3.6
4.0
2.0
1.1
1.8
1.25
1.4
1.6

1 of 1

DOE/ER/ 60844-3

EXPERIMENTAL ASSESSMENT AND MODELING OF INTERPHASE MASS TRANSFER RATES OF ORGANIC COMPOUNDS IN MULTIPHASE SUBSURFACE SYSTEMS

Final Report

Covering Period

July 1, 1989 through June 30, 1993

Principal Investigators

Linda M. Abriola, Ph.D. and Walter J. Weber, Jr., Ph.D., P.E.

Environmental and Water Resources Engineering

Dept. of Civil and Environmental Engineering

The University of Michigan

Ann Arbor, MI 48109-2125

October 1993

Prepared for

THE UNITED STATES DEPARTMENT OF ENERGY

AGREEMENT NO. DE-F602-89ER60844

Office of Health and Environmental Research

Subsurface Science Program

MASTER

DISTRIBUTION OF THIS DOCUMENT IS UNLIMITED

NOTICE

This report was prepared as an account of work sponsored by the United States Govenment. Neither the United States nor the Department of Energy, nor any of their employees, nor any of their contractors, subcontractors, or their employees, makes any warranty, express or implied, or assumes any legal liability or responsibility for the accuracy, completeness, or usefulness of any information, apparatus, product or process disclosed or represents that its use would not infringe privately-owned right.

ACKNOWLEDGMENTS

The authors thank Dr. Frank J. Wobber, Program Manager, Subsurface Science Program, Office of Energy Research, U. S. Department of Energy, for his support. This research was possible due to funding provided by the U.S. Dept of Energy under Grant #DE-F60289-ER60844. The authors also thank the students and research fellow who contributed to the research effort (in alphabetical order): Tim J. Dekker, Joyce S. Dunkin, Gregory D. Hoffman, Susan E. Powers, and Klaus M. Rathfeller.

Abstract

Results of an experimental investigation into steady state dissolution of nonaqueous phase liquids (NAPLs) entrapped within water saturated porous media are presented. The influence of porous media type, NAPL characteristics, and aqueous phase flow velocity are examined for transient and steady-state dissolution of NAPL. Entrapped NAPL distributions are examined and are found to influence mass transfer between the phases. A phenomenological model for the steady state mass transfer process is developed which expresses a lumped mass transfer coefficient as a function of the hydrodynamics of the system and grain size parameters as a surrogate measure of the NAPL distribution. Transient dissolution data is used to develop two alternative phenomenological models for mass transfer. The models are incorporated into a one-dimensional numerical simulator and are shown to be effective predictors of transient dissolution data in similar experimental systems.

In order to further explore the effects of scale and heterogeneities on NAPL dissolution, the sphere model is incorporated into a two-dimensional simulator and is used to explore long-term dissolution of a TCE spill in a layered system of sands. The simulation demonstrates the significance of heterogeneity, both in controlling the inital distribution of NAPL and the rate of NAPL dissolution.

TABLE OF CONTENTS

List of Figures iii
List of Tables iv
Executive Summary v

1.0 INTRODUCTION 1

2.0 BACKGROUND 4
2.1 Interphase Mass Transfer 4
2.2 NAPL Entrapment and Distribution 5

3.0 EXPERIMENTAL DESIGN 8
3.1 Materials 8
Porous Matrix Materials 8
Nonaqueous Phase Liquids and Solid Organic 9
3.2 Methods 13
Capillary Pressure-Saturation Curves 13
Column Experiments 14
Column Preparation 14
Steady State Dissolution Experiments 17
Transient Dissolution Experiments 19
Analytical Methods 20
Characterization of NAPL Distribution 21
4.0 RESULTS AND DISCUSSION 22
4.1 Pore structure and NAPL Entrapment 22
4.2 Steady State Dissolution Experiments 25
NAPLS 25
Development of phenomenological model 26
Naphthalene 29
4.3 Transient Dissolution Experiments 30
Experimental Results 30
Development of Phenomenological Model 34
Theta Model for Transient NAPL Dissolution 35
Model Development 35

Model Calibration 36
Model Verification 36
Sphere Model for Transient NAPL Dissolution 39
Model Development 39
Model Calibration 40
Model Verification 40
Alternate Transient Dissolution Models 43
5.0 TWO DIMENSIONAL NUMERICAL MODELING 45
6.0 CONCLUSIONS AND RECOMMENDATIONS FOR FURTHER RESEARCH 49

APPENDIX: List of Published Work and Presentations

LIST OF FIGURES

Figure 2.1.1	Typical capillary pressure saturation curves	7
Figure 3.1.1	Sand grain distributions	10
Figure 3.2.1	Experimental Set-up for Capillary Pressure-Saturation Measurements	15
Figure 3.2.2	Experimental Set-up for Column Dissolution Experiments	16
Figure 3.2.3	Approach of effluent concentrations to pseudo-steady state concentrations	18
Figure 4.1.1	Effect of grain size on pressure-saturation curves	24
Figure 4.1.2	Effect of grain size distribution on pressure-saturation curves	24
Figure 4.2.1	Effect of sand type on effluent concentration	25
Figure 4.2.2	Model fit for styrene dissolution rates	28
Figure 4.3.1	Example results from transient dissolution experiment	31
Figure 4.3.2	Effect of median grain size on transient styrene data	32
Figure 4.3.3	Effect of aqueous phase velocity on NAPL dissolution	33
Figure 4.3.4	Optimal theta model simulation of transient styrene data	37
Figure 4.3.5	Prediction of transient TCE dissolution with the theta model	38
Figure 4.3.6	Optimal sphere model simulations of transient styrene data	41
Figure 4.3.7	Prediction of transient TCE data with sphere model	42
Figure 4.3.8	Comparision of model simulations	43
Figure 5.1	Two-dimensional simulation domain	45
Figure 5.2	Two dimensional simulation results	48

LIST OF TABLES

Table 3.1.1	Porous Medium Properties	9
Table 3.1.2	Physical Properties of Organic Phases	12
Table 3.2.1	Summary of Steady-State dissolution experiments	18
Table 3.2.2	Experimental variables for naphthalene dissolution experiments	19
Table 3.2.3	Summary of Transient dissolution experiments with NAPLs	20
Table 4.2.1	Optimum models for description of NAPL dissolution rates for different pore structure parameter sets	27

Executive Summary

Results of an experimental investigation into steady state dissolution of nonaqueous phase liquids (NAPLs) entrapped within water saturated porous media are presented. The influence of porous media type, NAPL characteristics, and aqueous phase flow velocity are examined by means of a series of laboratory column experiments, both for transient and steady-state dissolution of NAPL. Nonequilibrium dissolution effects are observed in many of the experiments, resulting in column effluent concentrations less than the known solubility limits of the organics examined. Entrapped NAPL distributions are examined and are found to influence mass transfer between the phases. A phenomenological model for the steady state mass transfer process is developed which expresses a lumped mass transfer coefficient as a function of the hydrodynamics of the system and grain size parameters as a surrogate measure of the NAPL distribution. Transient dissolution data is used to develop two alternative phenomenological models for mass transfer. The theta model relates the mass transfer process to porous medium properties, Reynold's number and volumetric fraction of NAPL. The sphere model quantifies mass transfer coefficient and specific surface area independently, using results of steady-state napthalene dissolution experiments to calculate mass transfer coefficient and an idealized sphere geometry for calculation of interfacial area. The models are incorporated into a one-dimensional numerical simulator and are shown to be effective predictors of transient dissolution data in similar experimental systems.

In order to further explore the effects of scale and heterogeneities on NAPL dissolution, the sphere model is incorporated into a two-dimensional simulator and is used to explore long-term dissolution of a TCE spill in a layered system of sands. The simulator is run in conjunction with a multiphase flow simulator to generate an initial distribution of the organic phase. The simulation demonstrates the significance of heterogeneity, both in controlling the initial distribution of NAPL and the rate of NAPL dissolution. Bypassing of the low permeability formations is shown to result in a significant increase in time required for complete dissolution of entrapped NAPLs at the field scale.

1.0 INTRODUCTION

Contamination of the subsurface at many Department of Energy (DOE) sites has occurred from the release of nonaqueous phase liquids (NAPLs) at waste disposal facilities. Industrial solvents including trichloroethylene (TCE) and carbon tetrachloride (CT), as well as petroleum hydrocarbons have been found in groundwater samples collected from DOE sites (DOE, 1991). Remediation of NAPL spill sites has traditionally involved pumping as much of the free organic phase from the aquifer as possible (Testa and Wiengardner, 1991). A significant fraction of the NAPL is retained in the porous media, however, creating a long term source of pollution as the entrapped NAPL partitions directly into the aqueous phase by interphase mass transfer exchange processes (Schwille, 1988; Mackay *et al.*, 1985).

The extent of interphase mass exchange in NAPL contamination scenarios traditionally has been quantified using a local equilibrium assumption; that is, it is assumed that the concentration of a contaminant in any phase is defined in terms of its concentration in other phase(s) at the same spatial location by equilibrium partitioning relationships (Abriola and Pinder, 1985). Field data, however, frequently indicate that concentrations of solutes in groundwater at NAPL contamination sites are lower than their corresponding equilibrium values (Mackay *et al.*, 1985; Feenstra and Coburn, 1986; Mercer and Cohen, 1990). Such data suggest that some physical or chemical process limits the extent of mass transfer from NAPLs to aqueous phases. Alternative explanations and interpretations which have been advanced to explain the field observations include: i) rate-limited interphase mass transfer; ii) physical by-passing of mobile phases around contaminated regions due to relative permeability effects or aquifer heterogeneities; and iii) dependence of equilibrium solubilities on NAPL composition (Abriola, 1989; Feenstra and Coburn, 1986; Mackay and Cherry, 1989).

Some laboratory scale experimental studies of the transfer of organic species from NAPLs to water have supported the validity of the local equilibrium assumption at this scale (Fried *et al.*, 1979; Miller *et al.*, 1990; Parker *et al.*, 1990). Other investigations, however, have shown that non-equilibrium effects may play an important role in interphase mass transfer processes under certain conditions (Hunt *et al.*, 1988b; Geller, 1990; Razakarisoa *et al.*, 1989; Imhoff *et al.*,

1990; Borden and Kao, 1992). A variety of experimental approaches and procedures for NAPL entrapment have been used in the above studies which may account for the differences in conclusions reached. Unfortunately, most studies have involved limited ranges of matrix materials, organic compounds, and aqueous-phase flow velocities, thus producing limited data with which to quantify rates of interphase mass transfer.

Similar to the lab-scale experiments, contaminant transport models have incorporated mass transfer using either the local equilibrium assumption (Abriola and Pinder, 1985, Corapciogla and Baeher, 1987) or nonequilibrium kinetics (deZabala and Radke, 1986; Hunt *et al.*, 1988a; Powers *et al.*, 1991). For nonequilbrium mass transfer, most of these models assume that interphase fluxes can be characterized by the product of an appropriate driving force and a related coefficient which itself is the product of a mass transfer coefficient and the specific interfacial area across which mass transfer occurs. Some of these models employ existing correlations to evaluate the mass transfer coefficient, along with an estimated specific interfacial area based on an idealized NAPL geometry (deZabala and Radke, 1986; Hunt *et al.*, 1988a; Powers *et al.*, 1991). Others use a lumped coefficient which incorporates both the mass transfer rate and interfacial area (Dorgarten and Tsang, 1990; Sleep and Sykes, 1989; 1990). Models of the latter type have limited utility for predicting long-term dissolution processes in which interfacial area changes with time. A combined equilibrium and rate-limited or "two-stage" mass transfer model is presented by Borden and Kao (1992) to describe dissolution of a NAPL mixture. These modeling efforts collectively suggest that the interphase mass transfer of organic species may be a rate-limited process when: i) NAPL is distributed as large multi-pore blobs; ii) aqueous phase velocities are large (i.e., contact times are short); iii) NAPL saturations are low (Dorgarten and Tsang, 1990; Powers *et al.*, 1991; Hunt *et al.*, 1988a); or, iv) the mass fraction of soluble species in the NAPL is small (Borden and Kao, 1992). Expressions for mass transfer coefficients relevant to a particular system of interest are generally unavailable, and minimal data exist for estimation of interfacial areas. Thus, conclusions derived from these modeling efforts are only qualitative.

Because of the limited availability of data to quantify NAPL dissolution rates and qualitative modeling efforts, this research was designed to investigate dissolution on the lab scale and use the results to formulate mathematical and numerical models that would be useful in predicting the success of DOE remediation efforts. The objectives of this work were (1) to explore the validity of the local equilibrium assumption for partitioning of organic compounds into the aqueous phase; (2) to characterize the effects of variation in flow rate, porous media characteristics, wetting conditions, and organic liquid characteristics on the rates and extent of mass transfer; (3) to develop a general model to describe the kinetics of mass transfer; and (4) to incorporate experimental data into a numerical model useful for the prediction of the effect of rate limited transfer on aquifer remediation

2.0 BACKGROUND

2.1 Interphase Mass Transfer

Interphase mass transfer processes can be visualized as involving a series of several steps, of which one or more may be rate limiting (Weber, 1972; Weber *et al.*, 1991). For the dissolution of pure NAPLs, diffusion and convection of an organic species away from the interface of the organic phase into the bulk aqueous phase is generally considered to be rate limiting (deZabala and Radke, 1986; Pfannkuch, 1984). It is thus typically assumed that the net flux of a species (J) between phases can be expressed with a linear-driving force model, with the concentration driving force approximated as the difference between bulk aqueous phase concentration (C) and the concentration of a solute which would be in thermodynamic equilibrium with the solute concentration in the NAPL (C_s):

$$J = -k_f (C - C_s) \qquad (2.1.1)$$

Here the constant of proportionality, k_f, is termed the mass transfer coefficient. Additional details regarding the use of this type of equation for NAPL dissolution processes have been provided by Miller *et al.* (1990) and Powers *et al.* (1991). A more general discussion of mass transfer processes and models for subsurface phenomena has been given by Weber *et al.* (1991).

Correlations for estimation of mass transfer coefficients from known system properties are usually presented in terms of the dimensionless Sherwood number ($Sh = k_f l_c / D_l$), where l_c is a characteristic length and D_l is the free liquid diffusivity of the organic species in water. This dimensionless parameter is a measure of the relative rates of interphase mass transfer and molecular diffusion. In engineered systems, where the specific interfacial area is generally known, empirical relationships have been developed based on the Gilland-Sherwood correlation (Welty *et al.*, 1969):

$$Sh = a + b\, Re^m Sc^n \qquad (2.1.2)$$

in which a,b,n and m are empirical constants. Re and Sc are the Reynolds ($Re = r_w\, q\, l_o/\mu_w$) and Schmidt ($Sc = \mu_w / (D_l\, r_w)$) numbers, respectively, in which r_w is the aqueous phase density, μ_w is the aqueous phase viscosity, and q is the Darcy or superficial velocity.

2.2 NAPL Entrapment and Distribution

An understanding of the dissolution process requires knowledge of the processes impacting NAPL entrapment and how the geometry of the entrapped organic affects mass transfer. The entrapment of NAPLs within porous media occurs when capillary forces are sufficiently strong to overcome viscous and gravity or buoyancy forces (Wardlaw, 1982; Mohanty *et al.*, 1987). The volume of NAPL blobs entrapped within pore spaces is frequently expressed as a residual saturation (s_{n_r}) which is a ratio of entrapped NAPL volume to pore space volume. Values of s_{n_r} measured during field scale and laboratory experiments are typically in the range of 10-35% in saturated regions of unconsolidated media, with levels as high as 50% in low permeability media (Ng *et al.*, 78; Schwille, 1988).

The distribution of NAPL blobs within a porous medium is a function of pore geometry and fluid properties. Entrapped blobs in water-wet systems generally have concave interfaces and are formed within a single pore or several adjacent pore bodies (Schiegg, 1980). Blobs become isolated during NAPL migration, as the interface between phases become highly curved, and consequently unstable. Studies utilizing two-dimensional etched glass micromodels have shown that NAPL will tend to "snap-off" in individual pore bodies in soils having high pore-body-to-throat size ratios (pore aspect ratios) (Chatzis *et al.*, 1983; Li and Wardlaw, 1986). Singlets, which exist within one pore body and are formed by the snap-off mechanism, predominate in well sorted unconsolidated sands (Larson *et al.*, 1981). NAPL can also be trapped by a mechanism known as "bypassing" in regions having several adjacent large pore bodies connected by relatively large throats and surrounded by relatively small throats, such as might be found in a lens of coarse sand within a finer sand (Morrow, 1971). The geometry of blobs generated by this mechanism in real porous media is very complex, often encompassing several adjacent pore bodies and throats (Chatzis *et al.*, 1983).

Entrapment of NAPLs in three-dimensional systems has been studied with the use of fluids which can be solidified within pore spaces. Styrene, an aromatic hydrocarbon, has been solidified by polymerization in consolidated and unconsolidated media (Morrow and Chatzis, 1981; Conrad *et al.*, 1992). Analysis of the solidified blobs is generally accomplished by categorizing them by size. Morrow and Chatzis (1981) have shown that a majority of blobs (~60%) produced in an unconsolidated, uniform-size distribution sand pack occupy only one pore body, consistent with snap-off mechanisms. Conrad *et al.* (1992) have shown that NAPL distributed within a uniform fine sandy media exists in a wide variety of blob shapes, with most of the residual saturation held in large, branched ganglia. They hypothesized several implications of NAPL distributions on dissolution rates, although no data was available to verify these effects.

The geometry of the entrapped organic depends in part on the pore structure. Petroleum engineers and soil scientists historically have used capillary pressure-saturation (P_c-s_w) curves as macroscopic measures of pore structure for pairs of wetting and non-wetting fluids (Morrow and Harris, 1965; Morrow, 1970). P_c-s_w curves produced by incrementally increasing and decreasing the pressure on the non-wetting phase inherently manifest hysteresis, which is attributable to "ink-bottle" and "rain drop" effects (Dullien, 1979).

Typical capillary pressure-saturation curves are depicted in Figure 2.2.1. These curves can be characterized by s_{w_r}, the bubbling pressure, P_{c_b}, which is the pressure at which pores begin to drain, and the slope of the curve ($\partial P_c/\partial s_w$) near the curve's inflection point. These characteristics can be conceptually related to physical pore structure properties. Very flat curves ($\partial P_c/\partial s_w \sim 0$) are indicative of uniform pore size distribution, while steeply sloped curves are found in well graded media (Brooks and Corey, 1966). Analysis of flow in a simplified pore structure model consisting of constricted capillary tubes indicates that the pressure at which a pore will empty during drainage is representative of the pore throat radius (due to the ink-bottle effect), while the pressure at which a pore fills during imbibition is representative of a pore body size (Dullien, 1979). Although information about the pore structure properties that control entrapment is

implicitly embedded in the capillary pressure-curves, quantifying these properties from capillary measurements can be problematic (Tsakiroglu and Payatakes,1991).

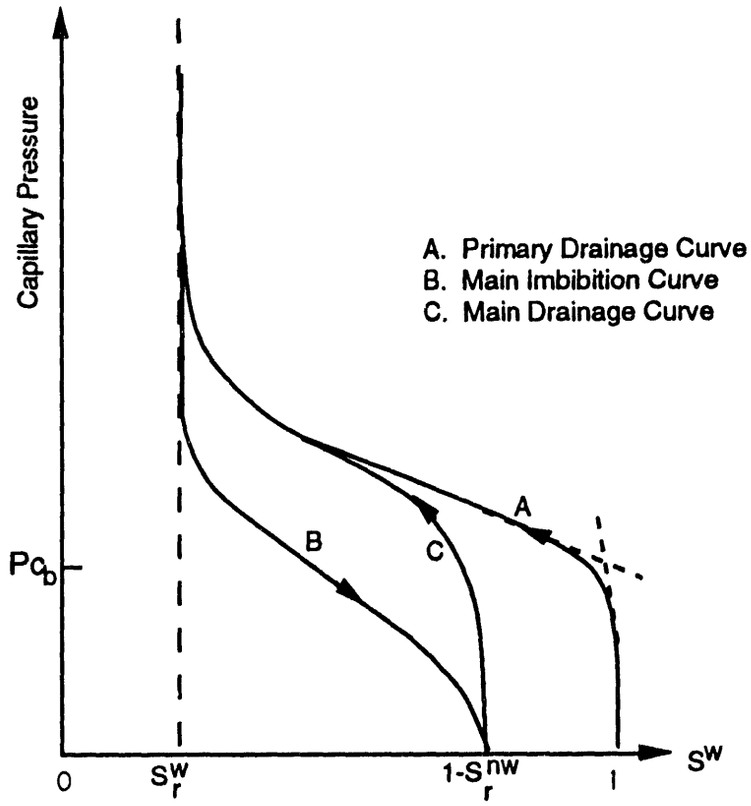

Figure 2.1.1 Typical capillary pressure-saturation curves

3.0 EXPERIMENTAL DESIGN

To accomplish the objectives of this work, four laboratory tasks were performed and two models were developed. The laboratory tasks included pore structure characterization experiments using air-water capillary pressure curves; steady-state dissolution experiments with entrapped NAPL and a solid organic phase; entrapped organic distribution experiments using polymerization techniques; and transient experiments with entrapped NAPLs . Phenomenological models were developed for steady state and transient experiments.

3.1 Materials

Porous matrix materials

Two general types of soils were employed: Ottawa sand, a uniform (#20-#30 mesh) silica sand purchased from Fisher Scientific, and Wagner soil, collected from a gravel pit in Ann Arbor, Michigan. The Wagner soil, from the Fort Wayne moraine, was deposited during the Wisconsin era of the Pleistocene Epoch (Kunkle, 1960). This unconsolidated unit is typical of aquifer materials in the Michigan area, which are predominantly of glacial origin. Wagner soil was sieved into uniform size fractions and washed with deionized water prior to use. All size fractions were comprised of very angular grains, representing a wide range of mineral components. Fractions retained on the #18 and #50 sieve were used as uniform sand isolates. Three mixtures of the sieved sand fractions were also used to investigate the influence of grain size distribution on NAPL entrapment and distribution. These media were characterized by their median grain size (d_{50}) and uniformity index ($U_i=d_{60}/d_{10}$), to represent the average and distribution of grain sizes (Driscoll, 1986). Here, 60% of the particles by weight have diameters smaller than d_{60}. Hydraulic conductivity was also measured for the uniform sands. A constant head permeameter method, as described by Bear (1972) was used for these experiments. Permeameters were 15-cm long by 5-cm diameter columns. Grain density measurements were conducted following the procedure outlined by Wray (1986). Properties of the uniform and

Table 3.1.1: Porous Medium Properties

POROUS MEDIUM	MEDIAN GRAIN SIZE (cm)	UNIFORMITY INDEX	HYDRAULIC CONDUCTIVITY (cm/s)	GRAIN DENSITY (g/cm^3)	POROSITY*
Wagner #50	0.045	1.45	0.075	2.67	0.392 ±0.013
Ottawa	0.071	1.21	0.12	2.65	0.327 ±0.024
Wagner #18	0.120	1.19	0.25	2.67	0.386 ±0.007
Wagner Mix #1	0.080	2.42	ND	2.67	0.381 ±0.012
Wagner Mix #2	0.082	3.46	ND	2.67	0.347 ±0.057
Wagner Mix #3	0.057	3.33	ND	2.67	0.346 ±0.017

* mean ± 95% confidence interval for given sand in replicate sand-packed columns
ND - not determined

mixed sand fractions used are presented in Table 3.1.1, grain size distribution curves are included in Figures 3.3.1a and 3.3.1b.

Nonaqueous Phase Liquids and Solid Organic

Styrene, (> 99.8% purity, Aldrich Chemical) a lighter-than-water NAPL, and trichloroethylene (> 99.8% purity, Fisher Scientific), a denser-than-water NAPL, are representative of compounds widely used by industry in the United States, and thus, there is a large potential for their improper disposal in the environment. Physical properties of these compounds which may affect their mobility and dissolution in subsurface environments are given in Table 3.1.2. Both compounds were dyed with 0.5 g/l of Oil-Red-O (Fisher Scientific), so that their respective flow and distribution patterns in porous media could be observed qualitatively. This dye ($C_{26}H_{24}N_4O$) is a weak surfactant and was found to alter interfacial properties of the organic phases. Styrene, as obtained from the manufacturer contains tertiary-butylcatechol (10-15 ppm) to prevent premature polymerization. Benzoyl peroxide (Fluka, Ronkonkoma, New York) was added at a level of 1% by weight to styrene immediately before steady-state rate experiments commenced to counteract the effects of the inhibitor and initiate polymerization of the styrene following dissolution measurements. Benzoyl peroxide was not added to styrene used in transient dissolution experiments.

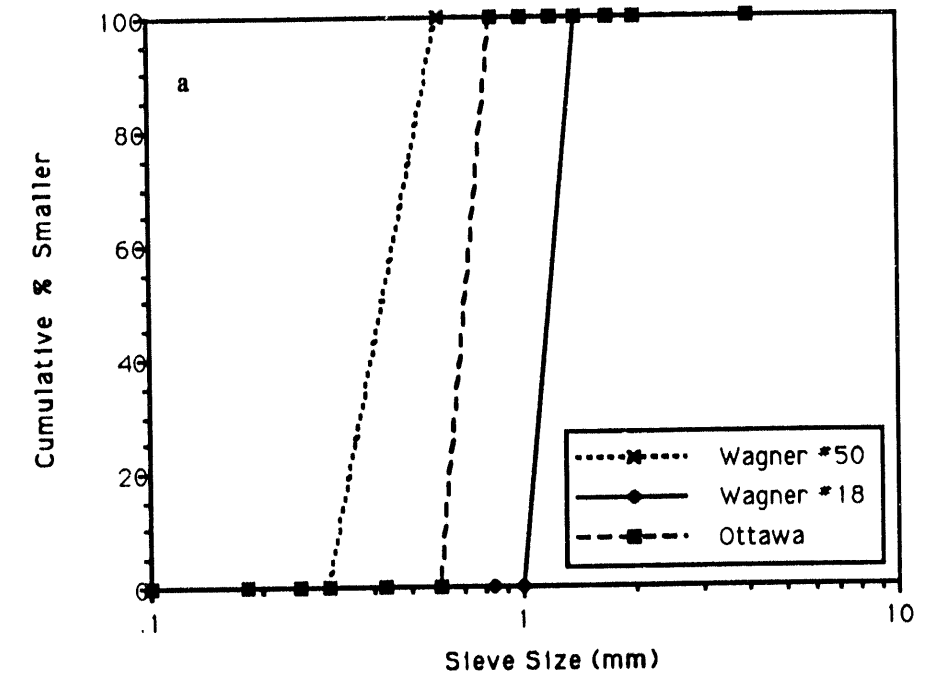

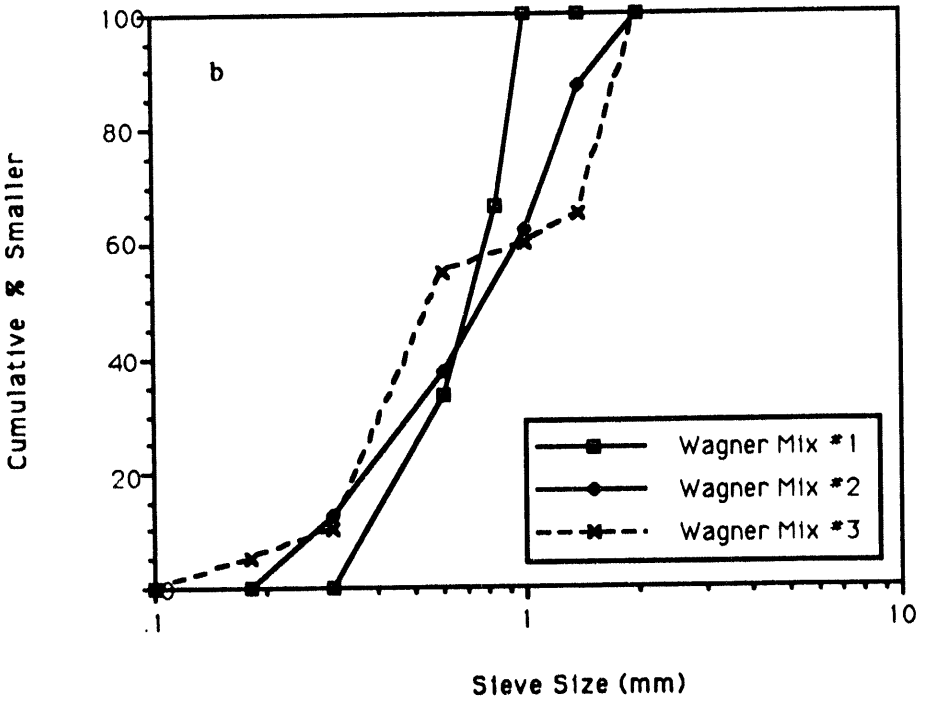

Figure 3.1.1: Sand grain distributions: a. uniform sands; and b. graded sands

For the steady-state experiments with solid naphthalene, spheres with a range of diameters were produced. Reagent-grade crystalline naphthalene (Fischer Scientific) was melted (110C) and formed into spheres by dropping the molten chemical from a capillary pipette through a 40-cm tall water column with a temperature decrease (85- 10C) over its length. The hot water at the top of the column allowed the molten naphthalene to assume a spherical shape as it slowly dropped through the water. The spheres solidified as they settled through the colder water at the bottom of the column. The solid spheres were gently sieved to segregate them into sets of equal size. Three different sets of spheres were produced with diameters ranging from 0.22 to 0.49 cm. Spheres smaller than this were not used because they sublimated rapidly, resulting in a variable surface area. A representative sample of each size faction was weighed and counter. The naphthalene surface area was then calculated assuming that perfectly spherical shapes were produced.

Surface and interfacial tensions were measured for each NAPL with a DuNoüy type ring tensiometer (Krüss USA, Model # K8, Charlotte, North Carolina) with a 9.545 mm platinum-iridium ring. As noted in Table 3, the addition of dye and benzoyl peroxide lowered the surface and interfacial tensions somewhat. A study of potential surface energy changes in styrene following the addition of benzoyl peroxide indicated that the surface tension did not change over a 24 hour period.

Solubilities of the dyed NAPLs in Milli-Q water (Millipore, Bedford, MA) were also measured. Approximately 30 ml of water and 2 ml of NAPL were introduced into a 40-ml screw cap vial and a Teflon-lined septum cap was tightly screwed onto the vial. After two days of equilibration and intermittent shaking, a syringe needle was inserted through the septum and all NAPL was removed from the aqueous phase surface. Aqueous phase samples were then collected and diluted into HPLC (high pressure liquid chromatography) grade methanol. Measured solubilities were within 10-20% of published values. The measured styrene solubility (230 mg/l) is less than the published value (290 mg/l) (Boundy *et al.*, 1965). TCE solubility showed the opposite trend; the measured value (1270 mg/l) was substantially higher than the

published value (1100 mg/l) (Verschueren, 1983). Presence of the dye may have affected the measured solubilities.

Table 3.1.2: Physical Properties of Organic Phases*

PROPERTY	SYMBOL	UNITS	TCE	STYRENE
Molecular weight	M	g/mole	131.5	140.1
Chemical formula			$CHCl{=}CCl_2$	$C_6H_5CH{=}CH_2$
Density	ρ	g/cm^3	1.47 (1)	0.908 (2)
Solubility	C^*	mg/l	1270 ± 12 (4)	230 ± 8 (4)
Surface tension (w/ air)	σ^{n-a}	dynes/cm	29(7) 28.8 ± 0.1 (3) 26.5 ± 0.0 (4)	32(2) 31.5 ± 0.6 (3) 24.2 ± 0.5 (4)
Interfacial tension (w/ water)	σ^{n-w}	dynes/cm	35(7) 29.6 ± 2.0 (3) 23.9 ± 0.5 (4)	35.5(8) 32.8 ± 0.0 (3) 28.0 ± 1.1 (4) 24.4 ± 0.6 (5)
Viscosity	μ	g/cm-s	0.0059 (1)	0.0073 (2)
Free liquid diffusivity (6)	D_L	cm^2/s	8.8×10^{-6}	8.0×10^{-6}

* Values ± 95% confidence interval, at 25 °C, unless otherwise noted

(1) Perry and Chilton, 1973
(2) Boundy *et al.*, 1965
(3) measured property (T=21-23 °C)
(4) measured, NAPL with oil-red-o dye (T=20-23 °C)
(5) measured, NAPL with dye and benzoyl peroxide (T=21 °C)
(6) Calculated from Wilke and Change (1955)
(7) Weast and Astle, 1981
(8) Dean, 1973.

3.2 Methods

Capillary Pressure-Saturation Measurements

P_c-s_w curves for the drainage and imbibition of water into the six sands investigated in this work were measured with commercially-available Tempe cells (Soil Moisture, Santa Barbara, California). Brass retaining rings, 3-cm high by 5-cm diameter, held the soil sample in contact with 0.5-bar pressure plates. Air pressure, provided from building utilities, was passed through a desiccant to remove moisture and was controlled with a pressure regulator (Gast Manufacturing, Benton Harbor, MI). A four-liter glass carboy provided excess volume in the air system to damp-out slight pressure variations. Air pressure was measured with a 150-cm Slack-Tube water manometer (Dwyer Instruments, Michigan City, IN), yielding accuracy of air pressure measurements to within a few millimeters of water. Water pressure was measured as the height of water in the serum collection vial with respect to the height of the bottom of the sand sample. Six Tempe cells were connected to the air supply in a parallel configuration to allow multiple measurements (Figure 3.2.1).

Air-dried soil was packed in the cells under vibration and saturated by passing at least 40 pore volumes of de-aired water through it. The cells were connected to the air system and the pressure increased to force water from the saturated soil. At least twelve hours were allowed between measurements to insure saturation had been reached. Water displaced from the Tempe cells was collected in serum vials, and saturations within the cells determined by gravimetrically monitoring change in the mass of the serum vials for each incremental change in pressure. Periodic measurement of the mass of the entire Tempe cell verified the accuracy of the saturation measurements. Duplicate or triplicate measurements of the primary drainage, main imbibition, and main drainage curves were made for each sand sample. Aqueous phase saturations at the completion of an experiment were verified by standard moisture content determination methods (Wray, 1986). Sand from the Tempe cells was dumped into a weighing boat, quickly covered

and weighed. After drying the sand in an oven at 105° C, the sample was reweighed and water content determined from the weight differential.

Column Experiments

Organic polymerization, steady state and transient experiments were performed in custom designed and manufactured one-dimensional soil columns, consisting of 5.5-cm ID glass tubing of 3-5 cm length supported by viton o-rings and stainless steel endplates. The endplates were lined with Whatman #42 filter paper or porous Teflon discs (Fluoroplastics, Philadelphia, PA), allowing either water-wetting or organic-wetting conditions at the end of the column during different phases of the experimental procedure. Tubing to and from the column was 1/8" Teflon or stainless steel to minimize interactions with the organic species. Stainless steel Swagelok fittings (H.E. Lennon, Farmington, MI) were used for all connections. Water flow to a column was controlled with a Rainin Rabbit HP pump (Rainin Instruments, Woburn, MA) fitted with a 25-ml/min pump head, while the NAPL was pumped with a mechanical syringe pump (Harvard Apparatus, Model #975, Natick, MA) through a 50-ml glass syringe (Figure 3.2.2).

Column Preparation

Experimental columns were packed under vibration. Degassed water, which had been distilled and purified in a Milli-Q filtration unit, was pumped through the column to insure saturation. A detailed description of the method can be found in Powers (1992). The top end plate was then removed and the paper filter replaced with a porous Teflon disk which had been soaked in the organic phase. With the top end plate back in place, NAPL was pumped to the column from the syringe pump at a rate of 0.42 ml/min (q~0.26 m/d). Styrene was pumped to the column in a downflow mode (TCE was pumped in an upflow mode) to achieve relatively stable displacements. The water-wet paper filter at the column bottom allowed the water to drain from the column during NAPL imbibition, but prevented the organic phase from exiting. NAPL was pumped until 75% of the pore space was filled with the organic phase. The flow of fluids was then reversed to displace the organic phase. Water was initially pumped at a low velocity

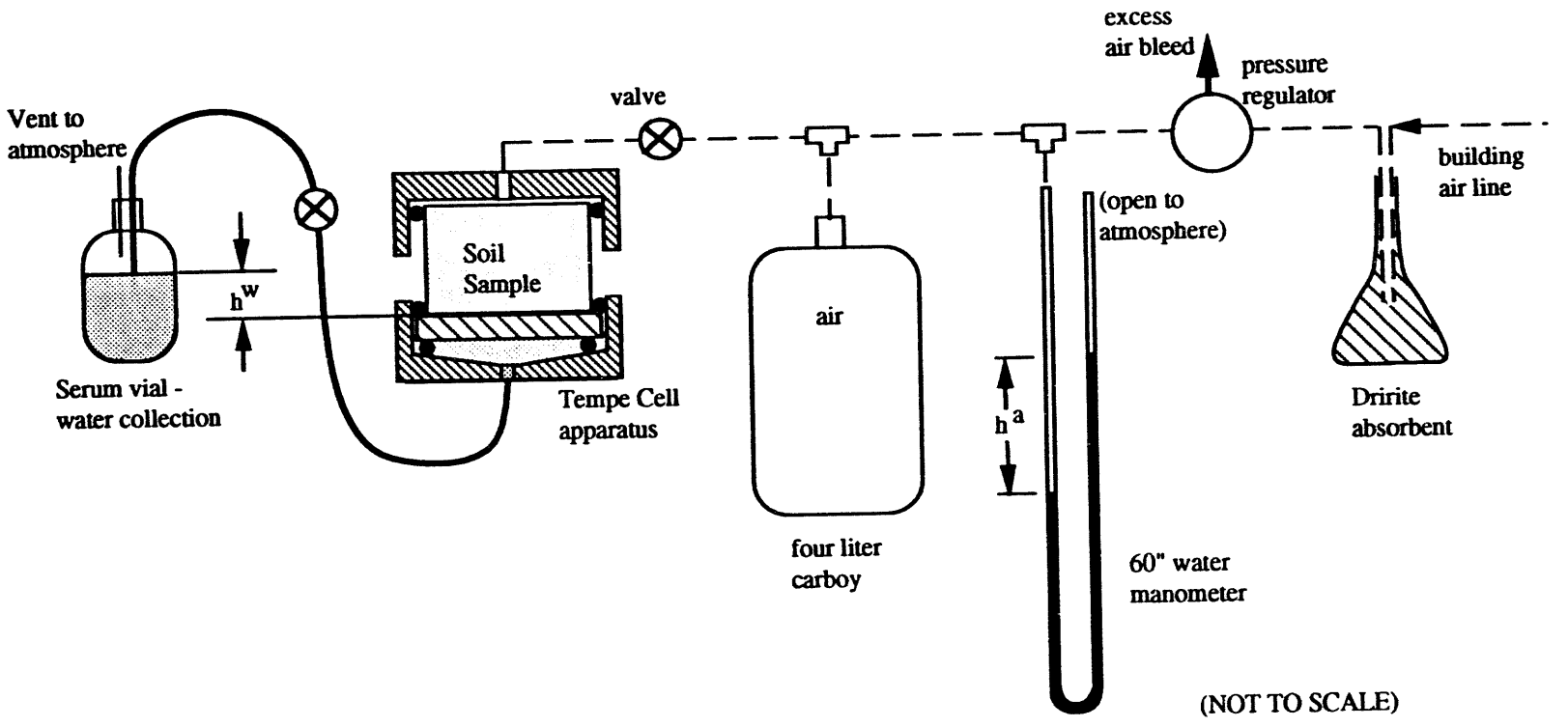

Figure 3.2.1: Experimental Set-up for Capillary Pressure-Saturation Measurements

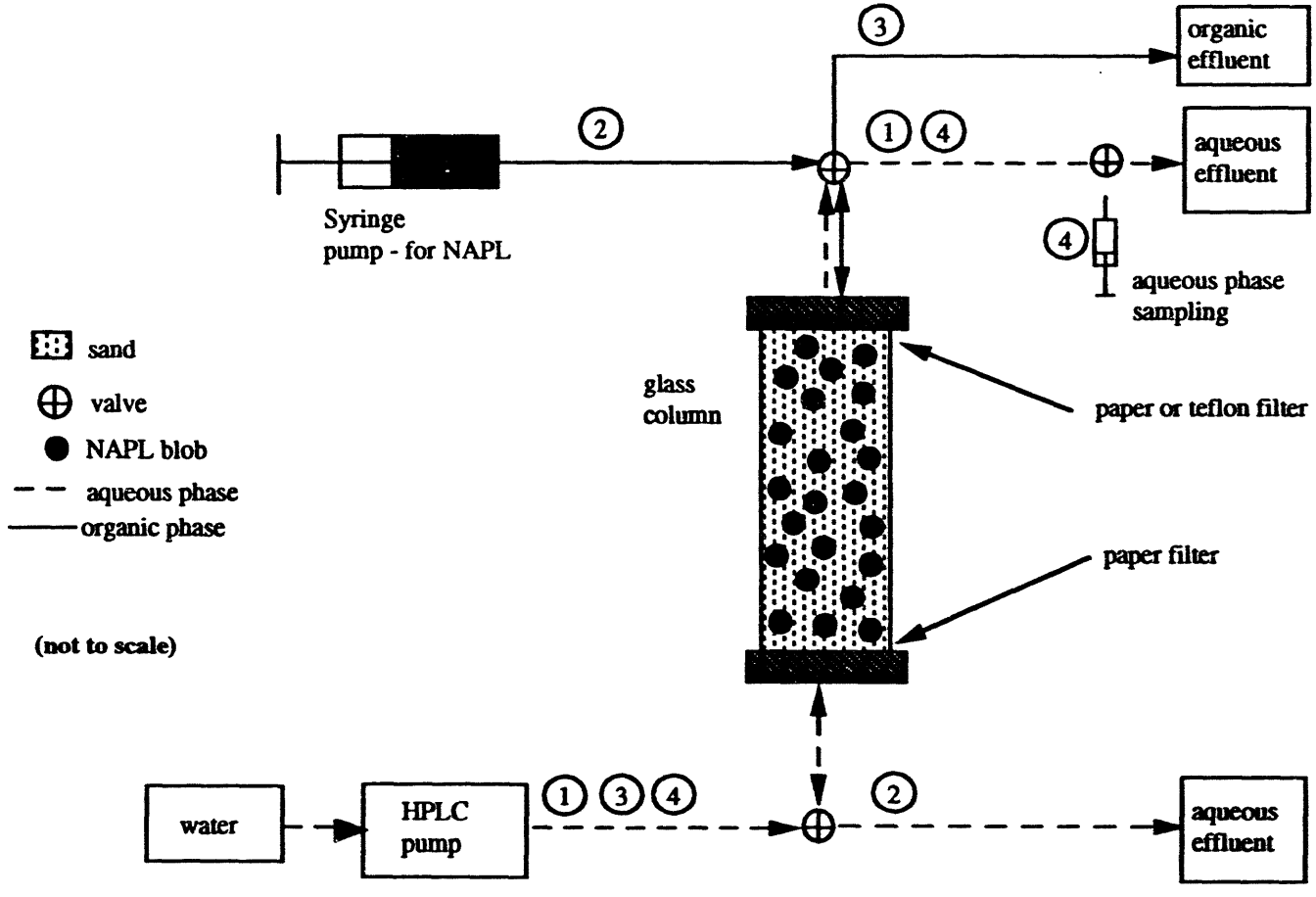

Figure 3.2.2: Experimental Set-up for Column Dissolution Experiments: 1) Saturate column with de-aired water; 2) Displace aqueous phase with NAPL; 3) Displace NAPL with water; and, 4) collect aqueous phase samples.

(q~0.3 m/d) until NAPL was no longer displaced. Flow to the column was then increased to the maximum velocity considered in the dissolution experiments (q~15 m/d) to obtain a minimum residual saturation in the column. Approximately three pore volumes of water were pumped into the column during the immiscible displacement of NAPL. Residual saturations are theoretically not affected by flow rate at these low Capillary numbers (Chatzis *et al.*, 1983). The porous Teflon disk was replaced by a paper filter at the end of the procedure to prepare for the dissolution experiments. Uniformity of the residual saturation was inspected during NAPL solidification experiments.

Steady-State Dissolution

Following establishment of a residual NAPL saturation, water was pumped through the column to measure dissolution rates under "steady-state" conditions. This condition was observed during the initial phase of dissolution, before a significant change in the interfacial area occurred. Figure 3.2.3 shows the approach towards steady-state effluent concentrations during one experiment. Approximately fifteen pore volumes of water were sufficient to reach steady state for the dissolution of styrene; ten pore volumes were found to be sufficient for TCE. After each steady-state condition was reached, the aqueous phase velocity was changed and the experiment continued.

Several velocities (4-5 for styrene, 2 for TCE) could be considered before a significant fraction of the NAPL was removed from the system. Here "significant" is operationally defined as 10% of the initial mass of entrapped NAPL, as determined by a mass balance. Within this range of saturation reduction, the variance between effluent sample concentrations in replicate columns containing the same sand and at a given flow rate was independent of the order in which that velocity was considered (i.e., first or third). Aqueous phase effluent samples were collected in triplicate from a syringe port each time steady-state conditions were achieved. Residual saturations were determined from the mass of polystyrene (measured during NAPL solidification experiments) and the mass of organic species removed from the column during the dissolution experiment. Table 3.2.1 summarizes the steady-state experiments.

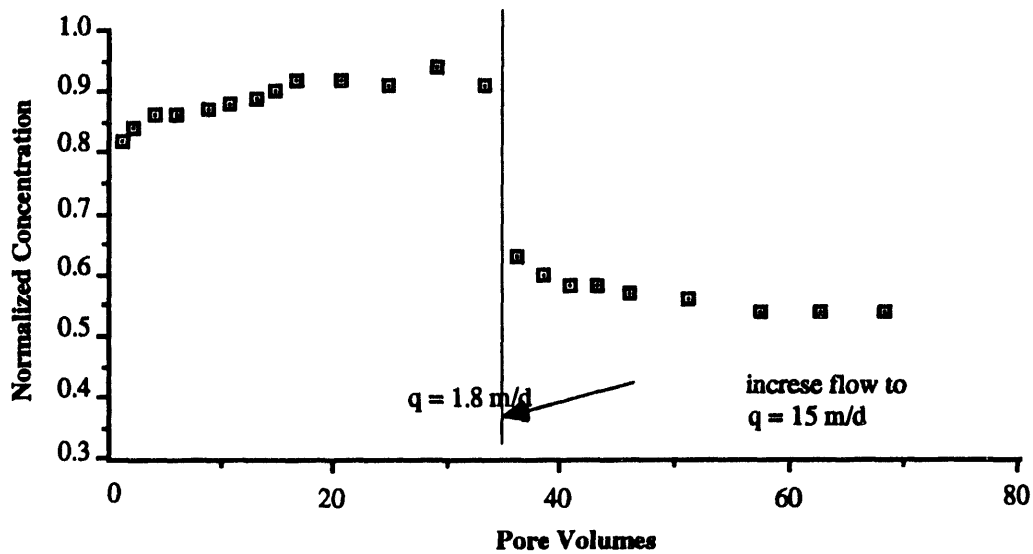

Figure 3.2.3: Approach of effluent concentrations to pseudo-steady-state concentrations (styrene dissolution from wagner #18 sand)

For the steady-state experiments with naphthalene (Table 3.2.2), a known mass of spheres was distributed throughout the column as dry sand was packed into the column under vibration. The in place volumetric fraction of naphthalene was calculated from the density of naphthalene and the column volume. The procedure used for the other transient experiments was then employed.

Table 3.2.1: Summary of Steady-State Dissolution Experiments

SAND	STYRENE		TCE	
	Range of Velocities (m/d)	Number of Columns	Range of Velocities (m/d)	Number of Columns
Wagner #50	1.5 -15	4	4.5 - 16	1
Ottawa	1.8 - 15	6	4.5 - 15	1
Wagner #18	1.5 - 15	3	3.8 - 15	2
Wagner Mix #1	1.5 - 15	3	7.4 - 16	3
Wagner Mix #2	1.5 - 15	2	--	0
Wagner Mix #3	1.5 - 24	3	--	0

An average of seven aqueous phase velocities were used for each experiment. Eighteen column experiments were conducted generating a total of 128 data points for use in the mathematical model development.

Table 3.2.2: Experimental Variables for Naphthalene Dissolution Experiments

Experimental Variable	Symbol	Range of Values
superficial aqueous phase velocity (m/d)	q	0.17 - 17
naphthalene volumetric fraction (–)	θ_n	0.015 - 0.088
naphthalene sphere diameter (cm)	d_s	0.22 - 0.49
median sand grain diameter (cm)	d_{50g}	0.045 - 0.17

Transient dissolution

Transient dissolution experiments (Table 3.2.3) were conducted to assess how NAPL dissolution rates change with time. The procedure for the establishment of a residual NAPL saturation before these experiments was the same as that described above for steady-state experiments. During the transient experiments, however, water flow to the column was continued at a constant rate for an extended period of time. For most experiments, duplicate aqueous phase samples were collected at regular intervals until analytical detection limits were reached; at this point, no organic phase remained within the column. These experiments were generally conducted for 2-6 days, depending on the NAPL solubility and aqueous phase flow. NAPL saturations were determined from the cumulative mass of organic species removed from the column with the aqueous phase. After disassembly of the column, the interior portions of the endplates were carefully observed to determine if any NAPL occupied the void spaces within the endplates. Results of such experiments were not considered valid.

Table 3.2.3: Summary of Transient Dissolution Experiments with NAPLs*

SAND	Darcy Velocity (m/d)	
	STYRENE	TCE
Wagner #50	3.5	--
Ottawa	3.8	7.6
	9.1	
Wagner #18	3.8	3.8
		15.2
Wagner Mix #1	3.8	7.4
	3.9	11.3
	6.1	15.8
Wagner Mix #3	6.1	--

* Indicated velocities are average Darcy velocities throughout experiment

Analytical Methods

Aqueous phase effluent samples collected during steady-state and transient dissolution experiments were immediately diluted in HPLC grade methanol (MeOH) (Fisher Scientific). Organic species concentrations in the MeOH-water mixture were determined by high pressure liquid chromatography. The HPLC system consisted of a Waters M45 solvent pump and Waters Lambda Max variable wavelength detector (Waters Chromatography Division, Millipore Corp., Milford, MA). The detector was interfaced with a Hewlett-Packard 3390A plotter-integrator (Avondale, PA), which automatically recorded retention time and peak area. A 25-cm column, packed with 5 μm C_{18} beads, was used for solute separation (Hypersil ODS C_{18}, Alltech, Deerfield, IL). Styrene was analyzed at a wavelength of 237 nm and TCE at 225 nm. A de-gassed 85% HPLC grade methanol, 15% Milli-Q water (by volume) mobile phase was used for styrene and TCE analyses.

Characterization of NAPL Distributions

Upon completion of steady-state dissolution experiments, columns containing styrene were subjected to high temperature and pressure conditions required to initiate the polymerization reaction (Wilson *et al.*, 1990). The column was removed from the experimental set-up and Swaglok plugs fitted over the fittings on each end of the column end plates. The column was then placed in an aluminum pressure cell and covered with water, after which the end plugs were removed, and the pressure cell lid attached with eight hexnut screws. The pressure within the cell was slowly increased to 80 psig using a pressurized cylinder of nitrogen gas. The entire pressure cell was then lowered into a hot water bath (80 °C) for approximately 48 hours, during which time the styrene was completely polymerized. Endplates were removed from the column and the sand-polystyrene mixture was gently flushed from the column and allowed to air dry. The dried sand-polystyrene mix was weighed to determine the mass, and hence residual saturation, of entrapped styrene. The methodology for separation and characterization of the different size fractions of the polymerized polystyrene can be found in Powers (1992).

4.0 RESULTS AND DISCUSSION

4.1 Pore structure and NAPL entrapment

NAPL residual saturations and blob size distributions were evaluated following polymerization of styrene trapped in the sand columns. Results of these experiments are presented in Powers, et al. (1992, 1993b). Measurements revealed that residual saturations were relatively insensitive to mean grain size for the medium sands. However, the degree of grading was found to impact residual saturation, with increased grading resulting in large residuals. These observations are consistent with those reported by others for organic residual saturations in uniform glass beads (Morrow and, 1981) and graded sands (Wilson et. al, 1990).

Qualitative characterization of blob size distributions was used to help analyze and explain trends observed in NAPL dissolution rates and residual saturations among the several porous media investigated. Sieve analyses of isolated NAPL blobs provided a qualitative measure of the volume percentage of NAPL entrapped as multi-pore ganglia. Geometrical considerations suggest that these ganglia have small specific interfacial areas relative to the high specific surface area of singlets. A significant fraction of NAPL entrapped in graded media was found to be distributed as multi-pore ganglia. These results are consistent with our understanding of the NAPL entrapment mechanisms, snap-off and by-passing, discussed previously. The absolute size of NAPL blobs was also found to be strongly dependent on grain size. Thus, even in media with uniform grain size distributions, specific surface areas, and by implication, lumped mass transfer rates, would be a function of median grain size.

The trends noted above regarding the dependence of entrapped NAPL blob size on porous media properties can be used to explain observations relating to the dependence of dissolution rates and residual saturations on type of porous media. It can be concluded that greater volumes of NAPL are entrapped within graded media due to the increased frequency of large-blob entrapment by the by-pass mechanism. Visual observation of blob distributions suggests that the higher residual saturations entrapped in graded media do not, however, necessarily correspond to a higher rate of mass transfer. In such media, specific surface area does not correlate directly with residual saturation due to retention of blobs of widely varying sizes.

Drainage and imbibition capillary pressure-saturation curves were measured for each of the media used in this study. The shape of these curves were quantified for use as a measure of pore structure characteristics, which define NAPL entrapment mechanisms and dissolution rates. Three different means for quantifying the shapes of these curves were employed; the Brooks-Corey (1966) and the vanGenuchten (1980) empirical relationships and a third method based on measurement of the bubbling pressure and the slope of a curve at its inflection point ($\partial P_c/\partial s_w$). Parameter fits to the data for these three approaches are summarized in Powers et al. (1992).

As would be expected from the theory of capillary flow phenomena, differences between the capillary pressure curves of different sands were indeed observed. Bubbling pressure increased with decreasing grain size for uniform sands (Figure 4.1.1), suggesting that the pore-throat sizes are smaller for fine grained media. The flat slope of the curves indicates that most of the water is released from the media within a narrow range of capillary pressures, suggesting that pore throat sizes are uniform throughout the media. A comparison of the slopes of curves presented in Figure 4.1.2 illustrates the effect of grain-size distribution among sands with comparable median grain diameters. Water is drained from the graded media over a wider range of capillary pressures, indicating that the pore-throat diameters have a broader distribution than in uniform media. Bubbling pressure heads of graded media are not correlated to the median grain size but seem to be a function of the range of grain sizes as well. This can be attributed to the fact that packing arrangements are much different in graded media; small grains can pack between larger grains, substantially altering the pore structure even though the median grain size is similar. The net effect is an overall decrease in pore throat size and correspondingly higher pressures are required to drain the media.

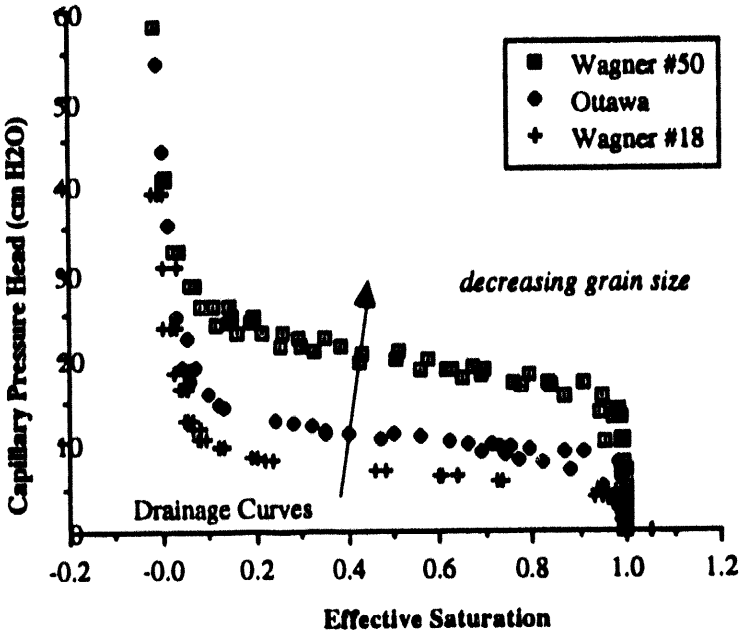

Figure 4.1.1: Effect of grain size on pressure-saturation curves

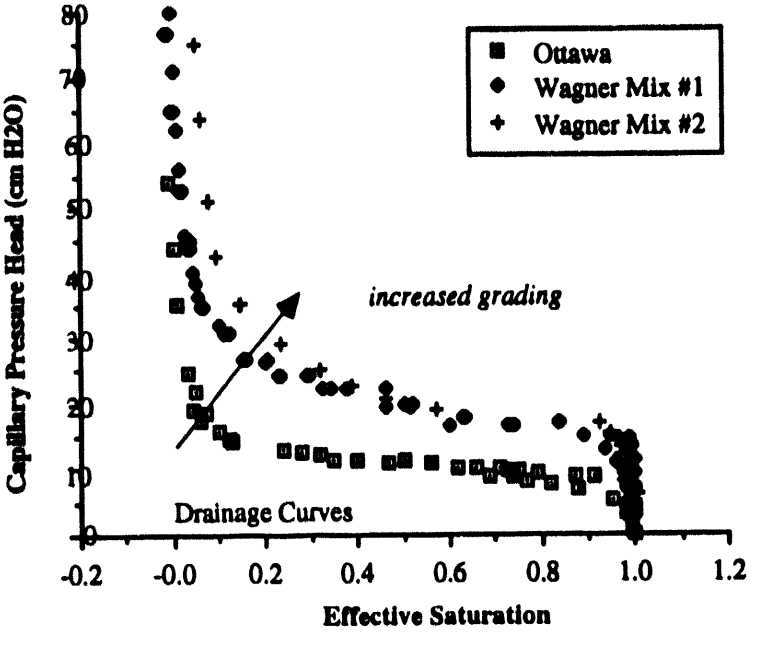

Figure 4.1.2: Effect of grain size distribution on pressure-saturation curves

4.2 Dissolution Experiments

NAPLs

Measurements from each dissolution experiment consisted of effluent concentrations and NAPL saturation for a prescribed sand type, aqueous phase velocity, and column length. Figure 4.2.1 presents results from some of the experiments. Here, normalized concentration (C/C_s) is plotted as a function of superficial (Darcy) velocity. This plot shows that effluent concentrations decrease with increasing velocity, and that there is a significant difference in effluent concentration for each sand type. For uniform sands of varying mean diameter (Ottawa and Wagner #50) the effluent concentration increased as the volume of entrapped NAPL (θ_n) increased. Miller *et al.* (1990) observed similar trends. This trend, however, was not observed for the Wagner #50 and Wagner Mix #1 sands. The graded sand retains a larger volume of NAPL but has lower effluent concentrations. This indicates a much lower mass transfer coefficient or specific interfacial area, or both, for the graded sand than for the uniform sand.

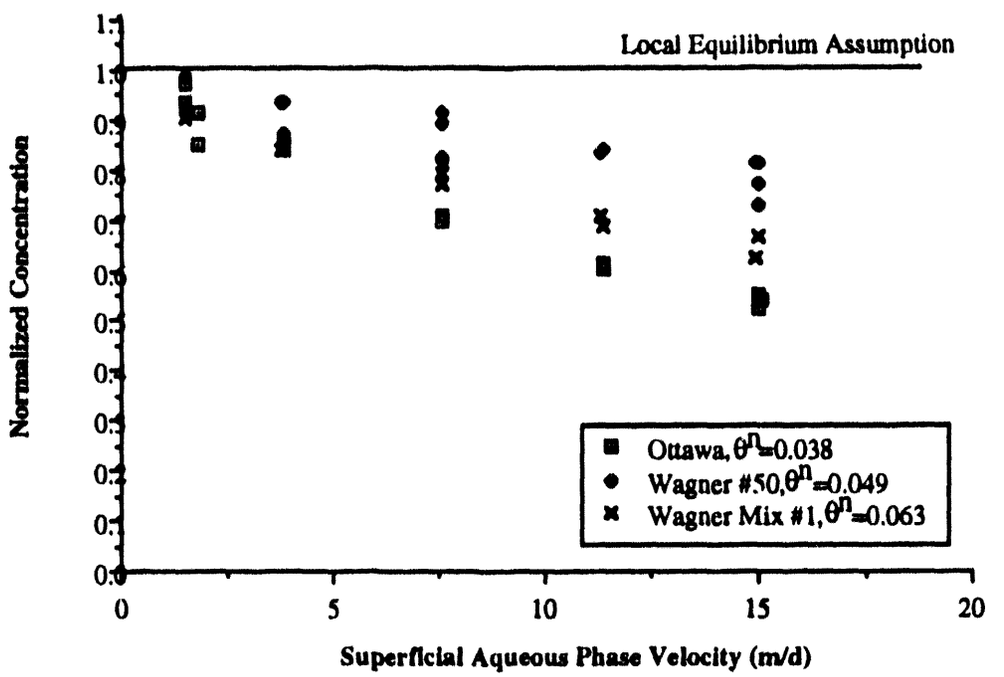

Figure 4.2.1: Effect of sand type on effluent concentration

Neglecting dispersion, the steady-state mass balance equation for the experimental system can be written with a linear-driving force mass transfer source term (1):

$$q \frac{dC}{dx} = -k_f\, a\, (C - C_s) \qquad (4.2.1)$$

Here q is the superficial (Darcy) velocity, and a is the specific interfacial area (surface area between the NAPL and the aqueous phase per unit volume of the matrix). Because the interfacial area was not measured, a lumped mass transfer coefficient ($\hat{k} = k_f\, a$), which is the product of the mass transfer coefficient and specific surface area, was evaluated. Solution of equation (3), subject to a boundary condition of C=0 at x=0; yields the following expression for the lumped mass transfer coefficient:

$$\hat{k} = -\left(\frac{q}{L}\right) \ln\left(1 - \frac{C}{C_s}\right) \qquad (4.2.2)$$

where L is the length of the column. Experiments resulting in effluent concentrations greater than 90% of the solubility limit were not used to calculate mass transfer coefficients because that parameter is highly sensitive to small errors in effluent concentration in this region.

Development of a Phenomenological Model

Data collected in the experimental phase of the work was incorporated into a phenomenological model describing steady-state NAPL dissolution rates. The modeling effort had two objectives: i) to determine which system properties most effectively characterize the dissolution process; and, ii) to generate a model having the capacity to predict dissolution rates in similar systems. Initial analysis determined that a simple relationship between the modified Sherwood and Reynolds numbers did not adequately describe the complexities of NAPL-water mass transfer rates in a variety of media. The modified Sherwood number which incorporates the lumped mass transfer coefficieny may be defined as (Miller *et al.*, 1990):

$$Sh' = \frac{\hat{k}\, d_{50}^2}{D_L} \qquad (4.2.3)$$

Alternative models considered used a Gilland-Sherwood type correlation (equation 2.1.2) to describe the dependence of the modified Sherwood number on the Reynolds number ($Re = \rho_w\, q\, d_{50}/\mu_w$) and some surrogate measure of the NAPL-water interfacial area. As summarized in

Table 5, parameters used as potential measures of surface area included: i) the volumetric fraction of NAPL entrapped in the system; ii) grain size distribution data; and, iii) drainage and imbibition parameters derived from the three methods for quantifying the capillary pressure saturation curves.

Combinations of the interfacial area parameters were systematically tested using a statistical software package, SYSTAT, to obtain estimates of the coefficients (b_i) for the log linearized form of a generalized Gilland-Sherwood type relationship:

$$\log(Sh') = b_0 + b_1 \log(Re) + \sum_{i=2}^{n} b_i \log(P_i) \qquad (4.2.4)$$

where P_i are parameters used to represent the surface area. The optimum combination of parameters for each surface area measure are summarized in Table 4.2.1. A detailed discussion of the statistical optimization approach is given in Powers, *et al.* (1992).

Table 4.2.1: Optimum Models for Description of NAPL Dissolution Rates for Different Pore Structure Parameter Sets

PARAMETER SET	MODEL	R^2	SEE *
NAPL Volumetric Fraction	$Sh'=18.4\ Re^{0.736}$	0.77	0.122
Grain Size Distribution	$Sh'=57.7\ Re^{0.611}\ d_{50}^{0.643}\ U_I^{0.413}$	0.94	0.062
P_c - s_w - vanGenuchten	$Sh'=340\ Re^{0.621}\ n_d^{-1.16}\ (\alpha_i/\alpha_d)^{-0.796}\ \alpha_d^{0.186}$	0.95	0.061
P_c - s_w - Brooks-Corey	$Sh'=20.7\ Re^{0.617}\ \lambda_d^{-1.10}\ h_{b_d}^{0.476}\ (h_{b_d}/h_{b_i})^{0.315}$	0.94	0.063
P_c - s_w - Slope & h_{b_d}	$Sh'=20.4\ Re^{0.596}\ slp_d^{0.884}\ h_{b_d}^{-0.982}$	0.94	0.061

* Standard error of estimate

Examination of the first model in Table 4.2.1 reveals that the modified Sherwood number is not correlated to the volumetric NAPL fraction at a high significance level. The other four models demonstrate that the Sherwood number is more highly correlated with the parameters describing pore structure. The excellent ability of these models to match experimental data supports the original hypothesis; i.e., that parameters linked to the pore-structure of porous media

can be used as representative measures of NAPL distribution and interfacial area. The results also indicate that grain size distribution, a very simple measure of pore structure, captures the effects of those pore structure characteristics which dictate NAPL entrapment processes as well as do more complex capillary pressure-saturation relationships.

An example of the quality of fit of the model to the experimental data is presented in Figure 4.2.2, which shows the relationship between experimental Sherwood numbers and Sherwood numbers estimated from a model utilizing grain size distribution characteristics. Analysis of the residuals between experimental and estimated Sherwood numbers reveals that there are no error trends related to either soil type or Sherwood number.

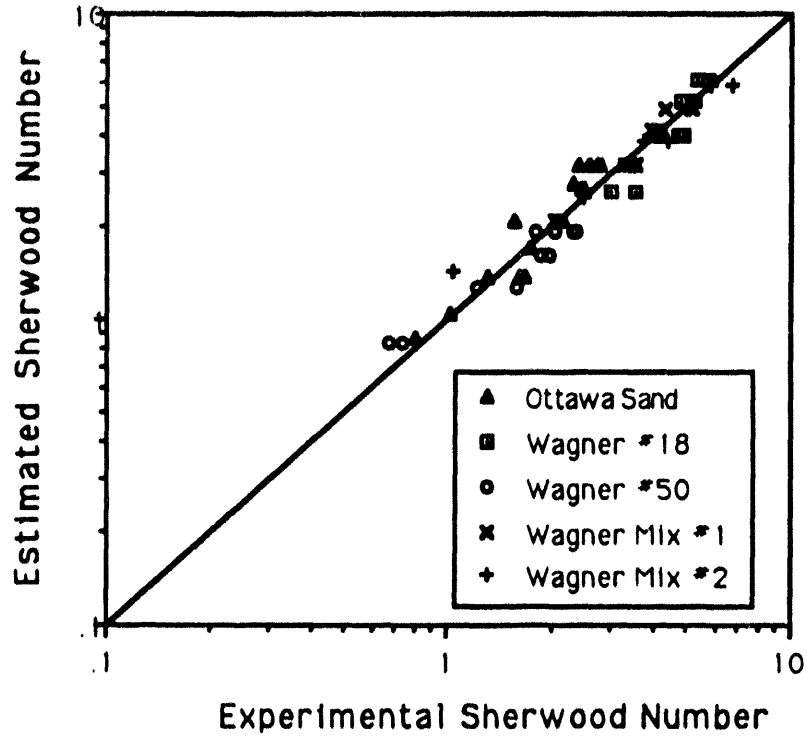

Figure 4.2.2: Model fit for styrene dissolution rates

To assess the relative abilities of the five models to predict dissolution rates under conditions other than those used for their development, additional dissolution experiments were conducted with TCE as the entrapped NAPL in three of the original sands and styrene as the

entrapped NAPL in a sixth type of sand (Wagner Mix #3). This media was a poorly-graded mixture, containing high percentages of very coarse and fine sands, and much smaller percentages of medium-coarse sands.

For TCE, the models predicted a somewhat higher rate of interfacial mass transfer than measured. On average, predicted Sherwood numbers are 1.4 times higher than experimental values. Consideration of th differences between free liquid diffusivities of TCE and styrene failed to account for these discrepancies. Another potential explanation of the discrepancy could relate to variations in NAPL distribution patterns between the two compounds. An experimental investigation including NAPLs with a wider range of solubilities would be required to explore this possibility. In general, however, the phenomenological models developed from styrene dissolution experiments provided reasonable estimates of TCE dissolution rates. For styrene dissolution in the Wagner Mix #3, the model incorporating the grain size distribution parameters was the most accurate.

It may be concluded from the above discussion that the correlation for the modified Sherwood number expressed in terms of the Reynolds number, mean grain size (cm) and uniformity index comprises the most appropriate phenomenological model for the NAPL dissolution experiments conducted in this study. A comparison of this model with other Sherwood number correlations reported in the literature for NAPL dissolution can be found in Powers (1992). In general, these other Sherwood number correlations were poor predictors of the NAPL dissolution observed in the present work.

Naphthalene

The results from the naphthalene sphere dissolution experiments consisted of a data base of effluent concentrations as a function of column length, sand type, sphere diameter, volumetric fraction of spheres and aqueous phase velocity. Mass transfer coefficients were calculated (eqn 4.2.1) from these data and incorporated into dimensionless Sherwood numbers ($Sh = k_f\, l/D_L$) where l is the characteristic length. Reynolds numbers, based on both the superficial (Re) and interstitial velocity (Re') were used to describe aqueous phase flow, and a ratio of sphere to sand grain size (d_b/d_{50})was used to represent relative blob size. Both sand grain diameter and sphere

diameter were considered as the characteristic length in the Reynolds and Sherwood numbers. Stepwise multiple regression analysis was performed to determine which of these dimensionless variables were correlated to the Sherwood number. Results of the regression analysis indicated that the models based on median sand grain diameter as the characteristic length were superior to those based on sphere diameters. It was determined that Sherwood numbers were not correlated to the column length, volumetric fraction or sphere size. Three equations were generated to describe naphthalene mass transfer coefficients statistically from the stepwise multiple regression analysis:

$$Sh = 81.7\ Re^{0.656} \qquad (R^2=0.83)(4.2.6)$$

$$Sh = 37.2\ Re'^{0.656} \qquad (R^2=0.83)(4.2.7)$$

and

$$Sh = 46.4\ Re'^{0.610}\ (d_b/d_{50})^{-0.218} \qquad (R^2=0.85)(4.2.8).$$

There was no statistical difference between the correlations based on superficial (eqn. 4.2.6) and interstitial (eqn. 4.2.7) velocities. Exponents for the Reynolds number are very similar to that determined for NAPL dissolution experiments ($Re^{0.61}$, eqn. 4.2.5). . This suggests that the hydrodynamics in columns containing naphthalene spheres emplaced within a sand pack are similar to those for columns containing entrapped NAPL blobs.

4.3 Transient Dissolution Experiments

Experimental Results

The results of the series of one dimensional transient column dissolution experiments show that time required for complete dissolution of entrapped NAPL is many times greater than predicted by equilibrium calculations. Figure 4.3.1 shows effluent concentrations from one of the column experiments, as well as the cumulative mass of NAPL removed with the aqueous phase over the course of the experiment.

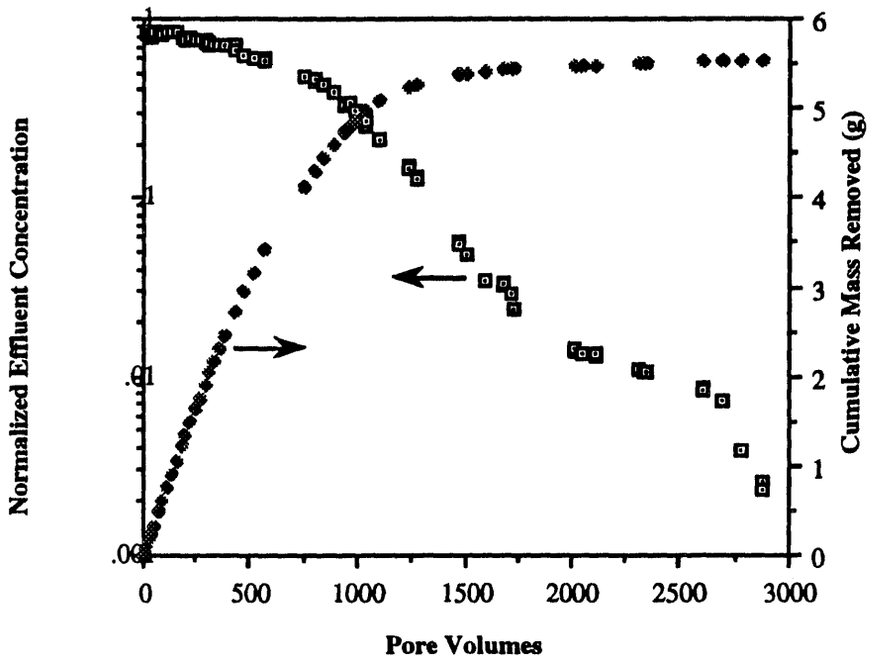

Figure 4.3.1: Example Results from Transient Dissolution Experiment

Reduced effluent concentrations at late times can be explained by the reduction in NAPL mass entrapped within the porous medium, and the corresponding decrease in total surface area across which mass transfer can occur. Similar findings were reported by Geller (1993, 1990) and Imhoff *et al.* (1990). The low concentrations required for drinking water guidelines and departures from local equilibrium observed in this and other studies suggest that any attempt to remove the very small mass of NAPL remaining within the column in order to meet drinking water quality standards will take a significant volume of water.

In an earlier section, it was shown that the distribution of NAPL blobs entrapped in a uniform porous media depend upon the median grain size, and it was hypothesized that this would have an effect on the rate of removal of NAPL due to the differences in NAPL-water surface areas associated with different NAPL blob sizes. Figure 4.3.2 presents data which support this hypothesis; experimental measurements of normalized effluent concentration for three uniform sands are compared to predictions based on the local equilibrium assumption. While the local equilibrium assumption might be considered adequate for the Wagner #50 sand,

predictions based on this assumption are certainly not representative of effluent concentrations for coarser media at the column scale. These trends can be explained by the occurrence of blobs with larger diameter, and hence smaller specific surface area, in the coarse sands compared with finer media.

The uniformity of grain sizes also affects dissolution rate characteristics over the course of remediation. Data from all experiments utilizing graded sands exhibited tailing of effluent concentrations to some degree. This suggests that the larger multi-pore-space blobs show limited dissolution at later times due to smaller specific surface area. Effluent concentrations from uniform sands, however, consistently showed exhibited uniform curvature.

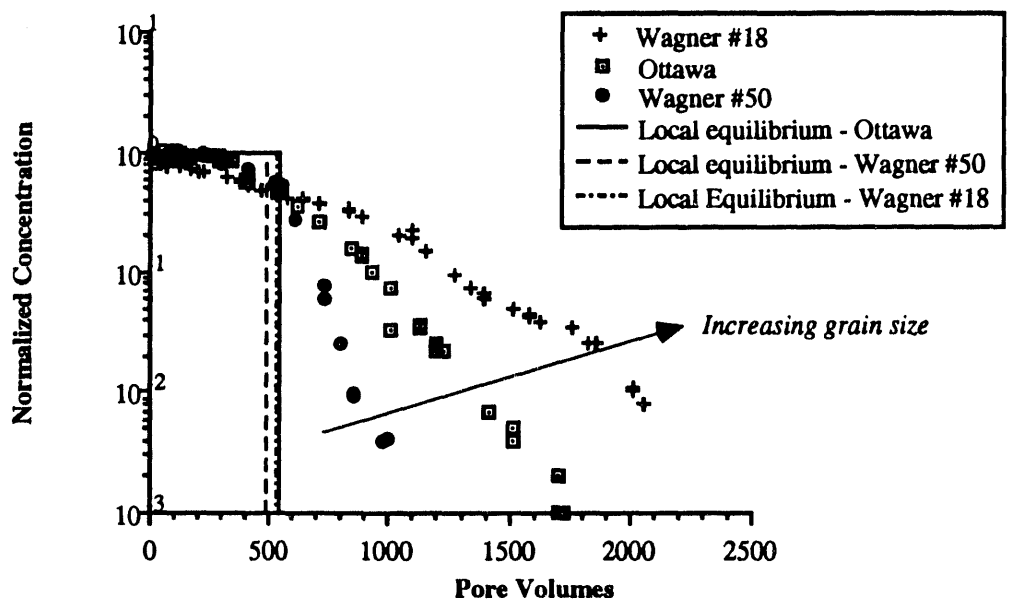

Figure 4.3.2: Effect of Median Grain Size on Transient Styrene

Results of steady-state dissolution experiments indicated that effluent concentrations decrease with increasing velocity due to a decrease in contact time between phases. The implications of this on remediation efforts are presented in Figures 4.3.3a and 4.3.3b. As anticipated from the steady-state results, the initial effluent concentration decreased with increasing aqueous phase flow rates (3.8 to 15.2 m/d). Thus, at the higher flow rates, mass

transfer limitations increased the total volume of water pumped through the column to achieve a specific reduction in aqueous phase concentrations (Figure 4.3.3a). Removal was much more rapid at higher flow rates, however (Figure 4.3.3b). Optimum aqueous phase velocities would, thus, have to be determined on the basis of costs and health risks associated with both pumping duration and volume of water requiring treatment. Further discussion of the above trends may be found in Powers *et al.* (1993a).

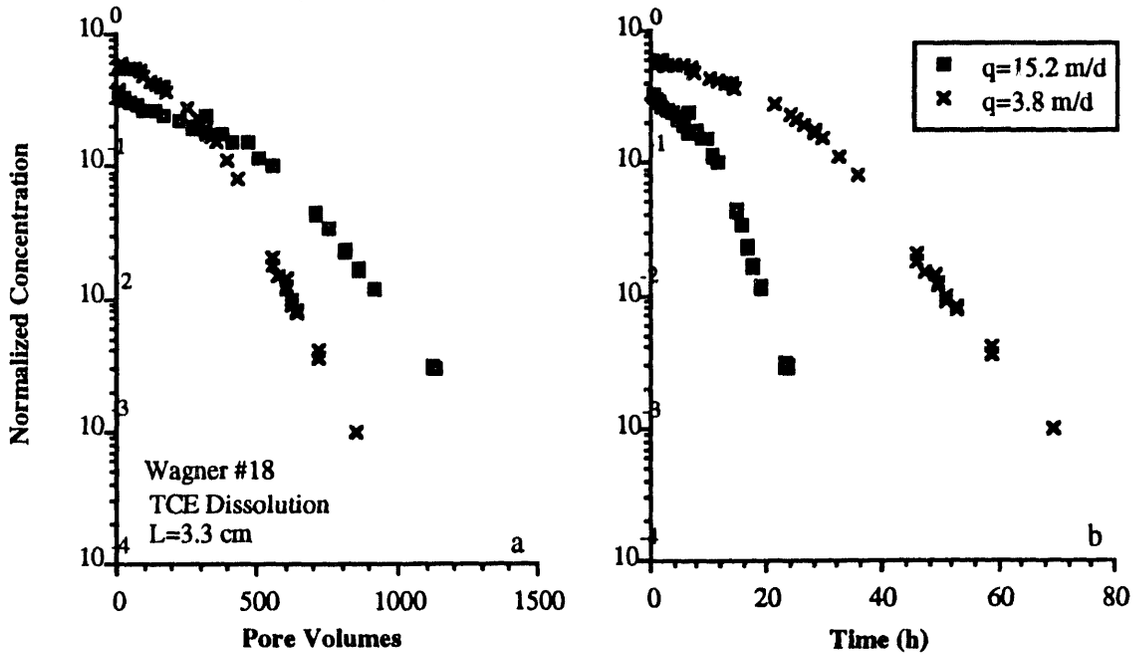

Figure 4.3.3: Effect of Aqueous Phase Velocity on NAPL Dissolution: a. Pore Volumes of Water; and, b. Time Required to Reduce Effluent Concentrations

The implications of the effects of sand type, solubility and aqueous phase velocity on remediation efforts are clear from the above discussion. Efficiency of clean-up operations, defined in terms of pore volumes of water pumped through the contaminated region requiring treatment, has been shown to decrease with increasing aqueous phase velocity, distribution of NAPL as large or multi-pore-space ganglia and low solubility NAPLs. Significantly more water was required to reduce effluent concentrations at the column scale than that predicted by equilibrium considerations. Although it is difficult to drw quantitative predictions of remediation efficiencies from these data, phenomenological models can be developed, to model

remedial alternatives under a wider range of conditions than explored by this sparse matrix of experiments.

Development of Phenomenological Models

Two conceptual models were developed to describe transient mass transfer rates over the course of removal of NAPL from the one-dimensional column systems. One model, the "theta model," treats the lumped mass transfer coefficient as a function of decreasing NAPL volumetric fraction. The second conceptual model describes blob distributions as a set of spherical globules with a range of diameters. This model, the "sphere model," utilizes independent equations for mass transfer coefficients and NAPL-water specific surface area. Assuming that a linear-driving-force model can adequately represent interphase mass transfer in sandy media, these mass transfer expressions can be incorporated into a one-dimensional partial differential equation describing spatial and temporal variations in aqueous phase concentrations due to NAPL dissolution processes (Powers *et al.*, 1991):

$$\theta_w \frac{\partial C}{\partial t} = \frac{\partial}{\partial x}\left\{\theta_w D_h \frac{\partial C}{\partial x}\right\} - q\frac{\partial C}{\partial x} + \hat{k}\,(C_s - C) \qquad (4.3.1)$$

where q is the superficial aqueous phase velocity; θ_w is the volumetric fraction of the aqueous phase and, D_h is the hydrodynamic dispersion coefficient. For the pure phase NAPLs used in this work, the aqueous phase concentration of solute in equilibrium with the NAPL, C_s, is defined as the organic phase solubility in water. The hydrodynamic dispersion coefficient is customarily represented for one-dimensional transport as (Bear, 1972):

$$D_h = \alpha_L \frac{q}{\theta_w} + \tau D_L \qquad (4.3.2)$$

where α_L is the longitudinal aquifer dispersivity and τ is the tortuosity.

The theta and sphere conceptual models were incorporated into a finite-element model, GANGLIA, (Abriola *et al.*, 1993) to simulate variable effluent concentrations as a function of water volume pumped through the column. This finite-element model solves the non-linear solute transport equation presented above. Values of non-linear coefficients are lagged one time step as described in Powers *et al.* (1991). The numerical accuracy of the developed simulator

was verified through comparisons with model predictions of the simulator presented in Powers *et al.* (1991).

Theta Model for Transient NAPL Dissolution

Model Development

The theta model was developed on the premise that, for any given porous medium, the change in lumped mass transfer coefficients as NAPL is removed from the system can be related to the volumetric fraction of NAPL in the system. Experimental results have shown that as the mass of NAPL in the system is reduced, concentrations decrease, implying that the lumped mass transfer coefficient must also be decreasing. Expanding upon the Gilland-Sherwood type equation developed for steady-state dissolution rates (eqn. 2.1.2), it was hypothesized that an expression of the form:

$$Sh' = \alpha\, Re'^{\beta 1}\, \delta^{\beta 2}\, U_i^{\beta 3} \left(\frac{\theta^n}{\theta_o^n}\right)^{\beta 4} \qquad (4.3.3)$$

could describe transient mass transfer rate coefficients. Here α, β_1, β_2, and β_3 were given in Table 4.3.1 (third equation), and θ_o^n is the initial volumetric fraction of NAPL in the system. The coefficient β_4 was assumed to be dependent on blob shape, and therefore on porous medium type. Since interstitial velocities also change during transient dissolution processes, dependence of the modified Sherwood number on a Reynolds number defined in terms of interstitial velocity ($Re' = Re\,(\varepsilon\, s^w)^{-1}$) rather than superficial velocity was used.

This correlation for modified Sherwood numbers was rearranged to provide an expression for a lumped mass transfer coefficient, ($\hat{k} = Sh'\, d_{50}^2/D_L$), and was incorporated into the finite-element model GANGLIA. Values of the volumetric fraction of NAPL, and hence mass transfer rate, were lagged one time step in this formulation. Small time steps (~0.1 hours) were used to ensure that the rate of change of saturation within each element was very small over each time step. Global mass balance error never exceeded 1%.

Model Calibration

Assessment of the β_4 parameter indicated that model simulations were highly sensitive to the value of β_4 over the range of 0.5 to 1.0 predicted by geometrical considerations. Actual values of β_4 appropriate for transient NAPL dissolution were obtained through calibration of the code to transient styrene data sets. Optimal fits of the styrene dissolution data, presented in Figures 4.3.4a and b, show that the theta model is capable of reproducing the trends observed in the data. Multiple linear regression analysis indicated that β_4 values can be correlated to the normalized median grain size ($\delta = d_{50}/d_M$) and uniformity index of the sand ($R^2 = 0.97$):

$$\beta_4 = 0.518 + 0.114\,\delta + 0.10\,U_i \qquad (4.3.4)$$

Here d_M is taken as the diameter of a "medium" sand grain (d_M=0.05 cm), as defined by the United States Department of Agriculture (Driscoll, 1986).

Model Verification

The correlation for β_4 coefficient values (eqn. 4.3.4) was incorporated into the numerical simulator to predict effluent concentrations from TCE dissolution experiments. It was generally found that this model, which was based on styrene dissolution data, is a good predictor of TCE effluent concentrations. Figures 4.3.5a and b present predictions for uniform and graded sands respectively. Discrepancies between the theta model and characteristic trends in effluent concentration data from uniform sands discussed above also apply to prediction of TCE effluent concentrations. That is, the model prediction has greater curvature as concentrations decrease than exhibited by the data (Figure 4.3.5a). The general trends in decreasing effluent concentrations observed in graded sands (Figure 4.3.5b) are well represented by the theta model. The tailing characteristic of the effluent concentrations from graded sands is not entirely captured by the theta model. A lack of data in the low concentration region makes it difficult to assess the significance of this discrepancy.

Experiments were not conducted to assess the validity of the theta model for a sand other than those utilized for model development. Further discussion of the applicability of the theta model can be found in Powers *et al.* (1993a).

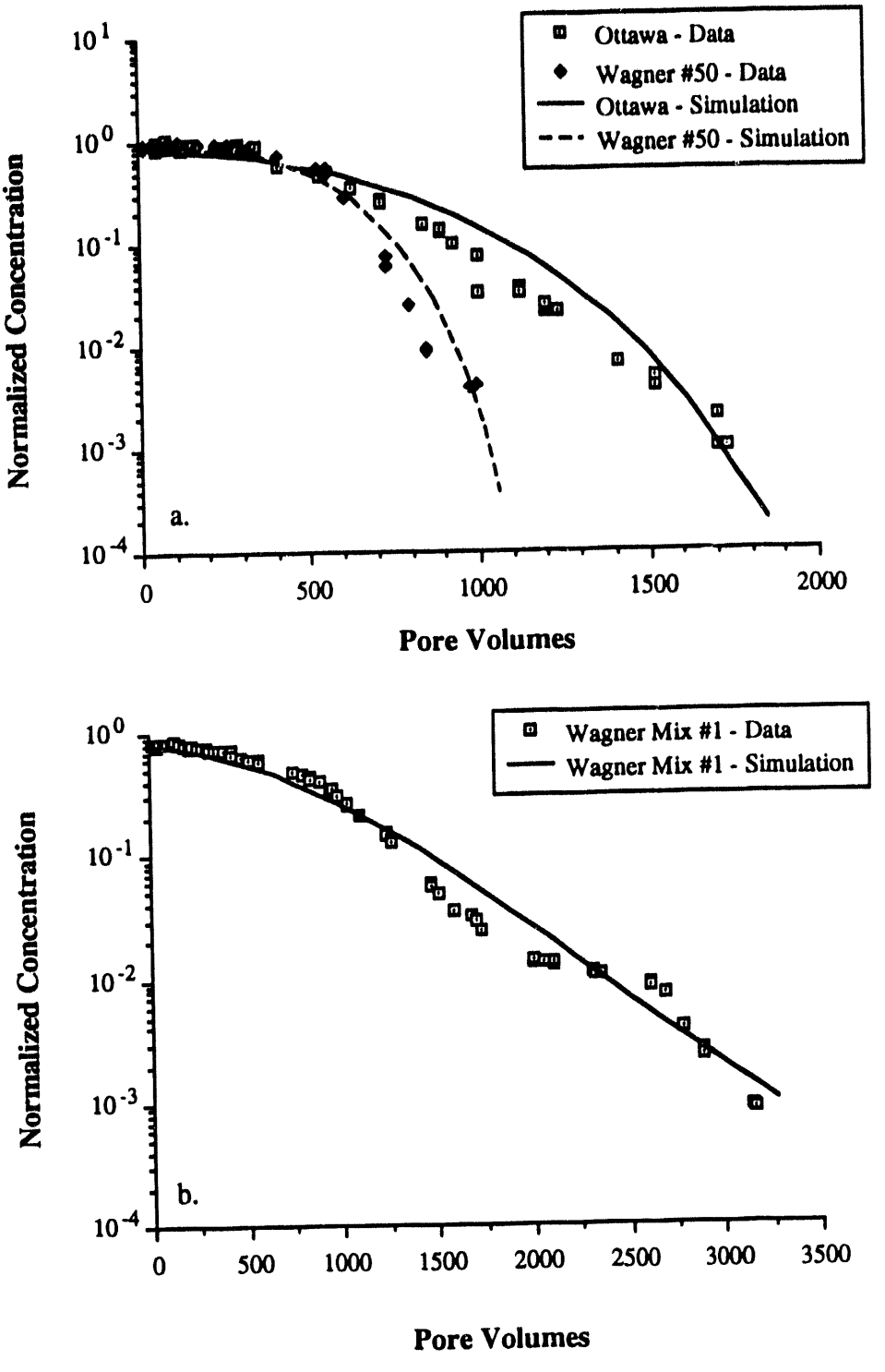

Figure 4.3.4: Optimum Simulation of Transient Styrene Dissolution Data with Theta Model: a. Uniform Sands; and, b. Graded Sands

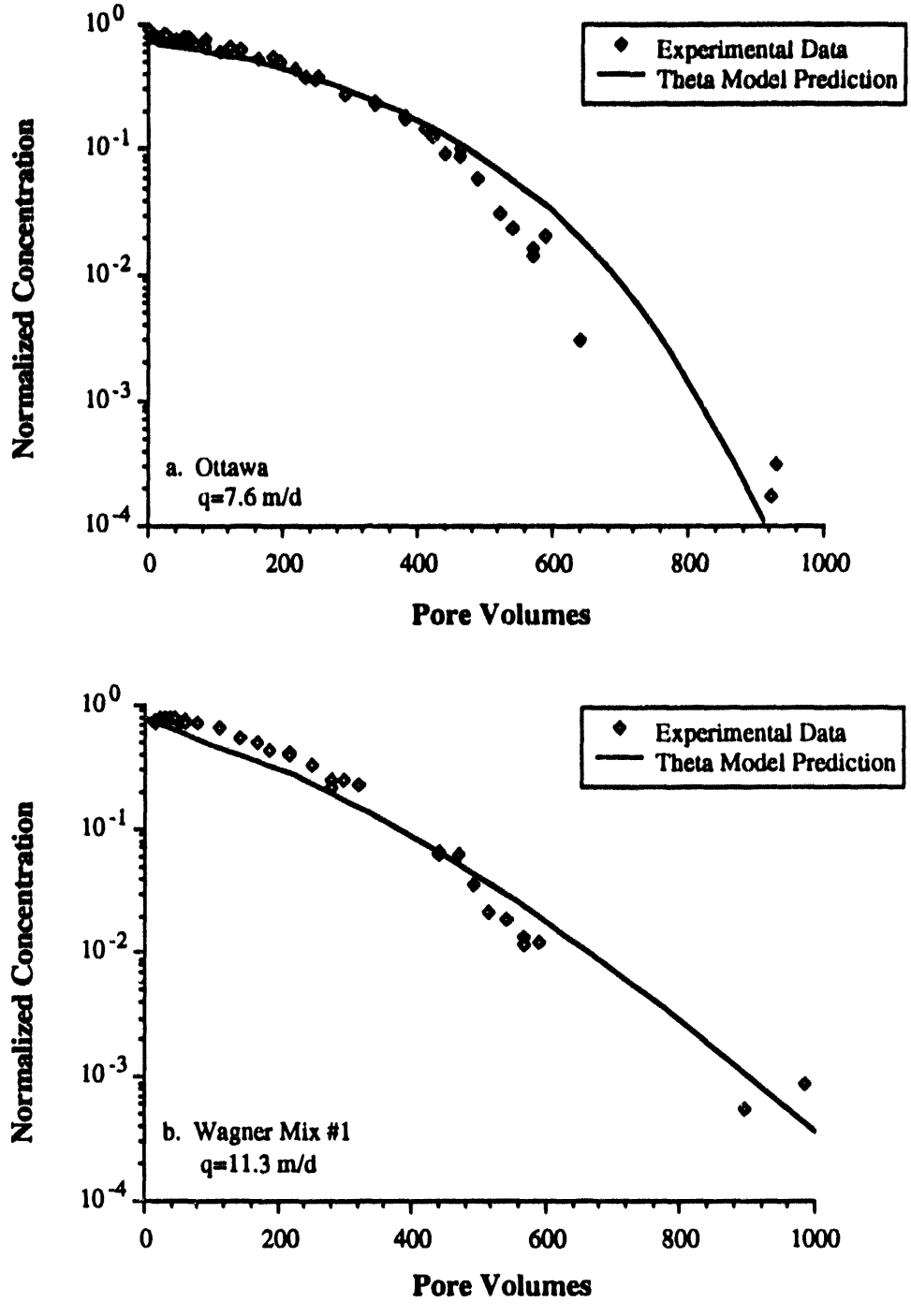

Figure 4.3.5: Prediction of Transient TCE Dissolution with Theta Model: a. Uniform Sand; and, b. Graded Sand

Sphere Model for Transient NAPL Dissolution

Model Development

The sphere model was developed with data independent of the transient dissolution data presented above. The basis of this model was the hypothesis that NAPL dissolution could be modeled with a linear-driving-force mass transfer expression (2.1.1) in terms of independently defined mass transfer coefficients and specific surface areas. This approach follows that described by Powers *et al.* (1991). In this case, however, NAPL blobs were modeled as spheres with a range of diameters rather than as equally sized spheres throughout. The methodology for determining specific surface area and mass transfer coefficients are described below.

Representative sphere dimensions for use in this model were based on polystyrene blob distrubution studies discussed in section 4.1. Diameters determined experimentally were used along with the mass (or volume) fraction of each size (f_r^i) to describe the distribution of NAPL for the sphere model. The specific surface area (a_o) was calculated as:

$$a_o^{sphere} = \sum_{i=1}^{n} \frac{3 f_r^i s^n}{\varepsilon R^i} f_m^i \qquad (4.3.5)$$

where n is the number of size ranges considered, R^i is a representative sphere radius within size range i, and f_m^i is a calibration parameter to describe discrepancies between actual blob shape and the idealized sphere geometry and to account for the fact that only a fraction of surface area is exposed to mobile water. The porosity term in the denominator was included only for those blobs which were large enough to incorporate sand grains within the total blob volume. Porosity was excluded from this expression for blobs expected to occupy one or two pore bodies. Over time, as NAPL is removed from the column, the blobs' radii and surface areas change. Incorporation of this transient surface area is critical for model development.

The sphere model as presented here is based on the correlation developed from naphthalene dissolution experiments in terms of Sherwood number as a function of Reynolds

number based on interstitial velocity (4.2.7). Use of this correlation accounts for the changing pore-water velocity over time as the blobs shrink.

Model Calibration

The mass transfer coefficient correlation (4.2.7) and the expression for sphere surface area (eqn. 4.3.5) were incorporated into the numerical code GANGLIA in order to simulate effluent concentrations for column experiments. These parameters change with time as NAPL is removed from the column, and calculation of these parameters was lagged one time step behind calculation of nodal concentrations.

The parameter f_m^i was used to calibrate the model using the styrene dissolution data. Sphere model simulations based on f_m values which were fit to experimental data sets did an excellent job of describing data over the course of time required to remove NAPL from column systems (Figures 4.3.6a and b). The data from graded sands (Figure 4.3.6b) showed characteristic changes in the slope of the data. This behavior has been interpreted as time periods controlled by dissolution of different blob sizes. The sphere model also predicts these changes in slope as small blobs, and then larger blobs, disappear from the system. Although the overall trend of the model simulation is consistent with data, the actual curvature of data is not followed.

Model Verification

Average values of f_m were used with the sphere model to predict effluent concentrations for TCE dissolution experiments to verify the model. Two different averages were considered for prediction of each TCE experimental data set: the average f_m value from calibration of all styrene dissolution data sets (f_m=0.72), and the average value of f_m within each type of sand. Since mass and size distributions of effective spherical blobs are also required as input parameters, this model is only capable of predicting NAPL dissolution from sands for which styrene emplacement, polymerization and blob size analysis has been conducted.

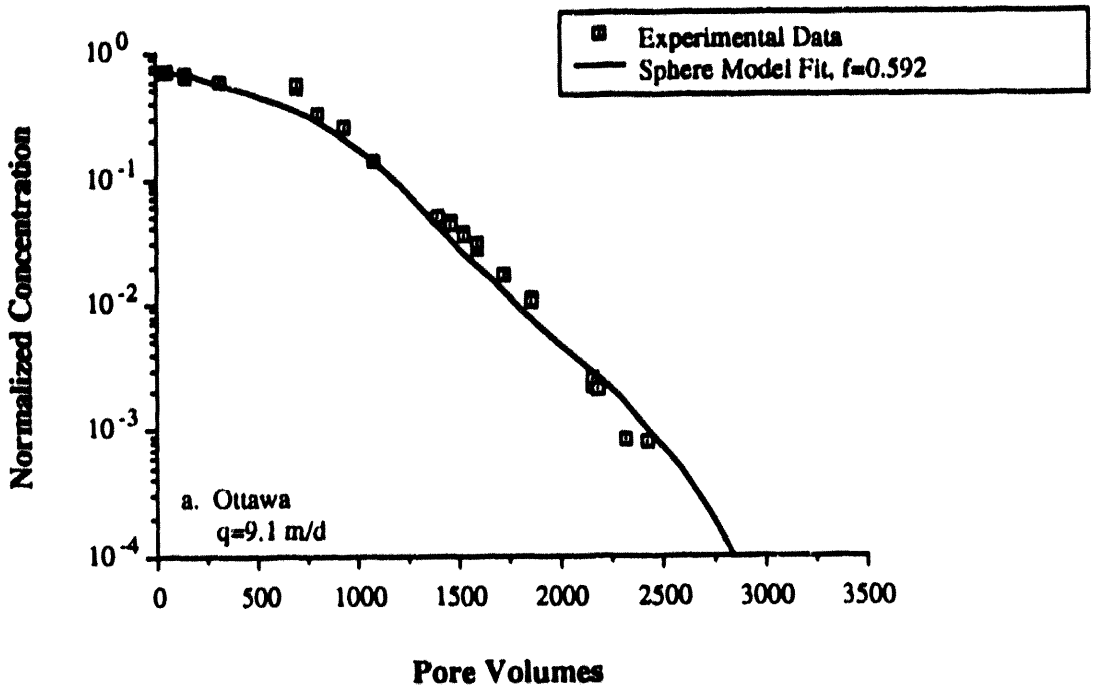

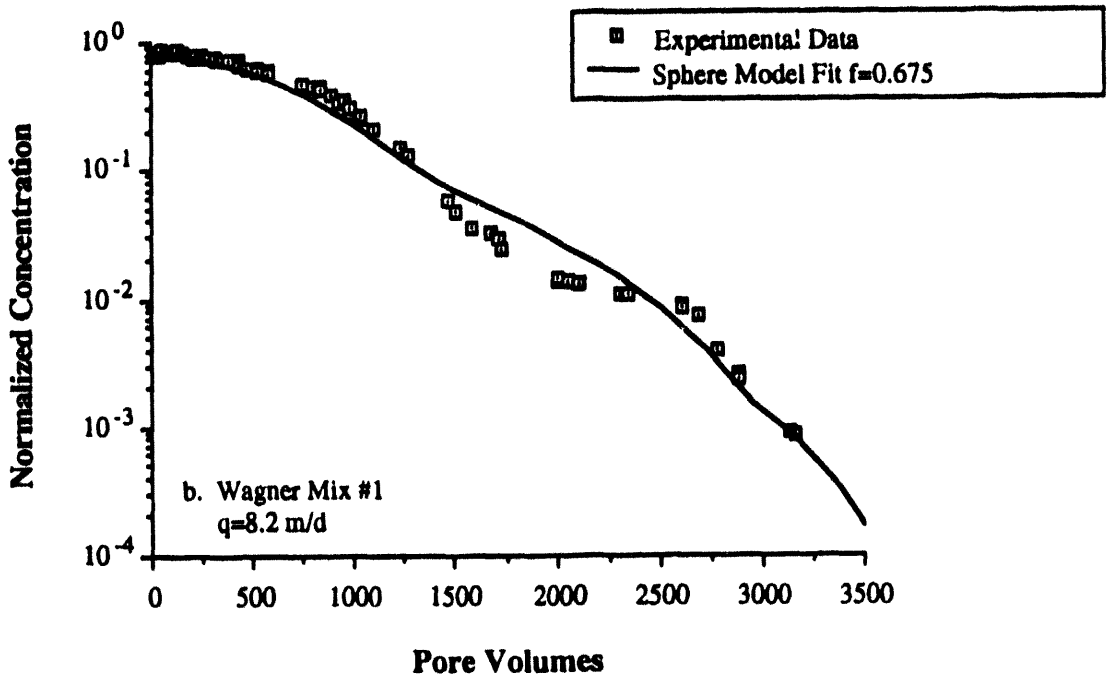

Figure 4.3.6: Optimum Simulation of Transient Styrene Dissolution Data with Sphere Model: a. Uniform Sand; and, b. Graded Sand

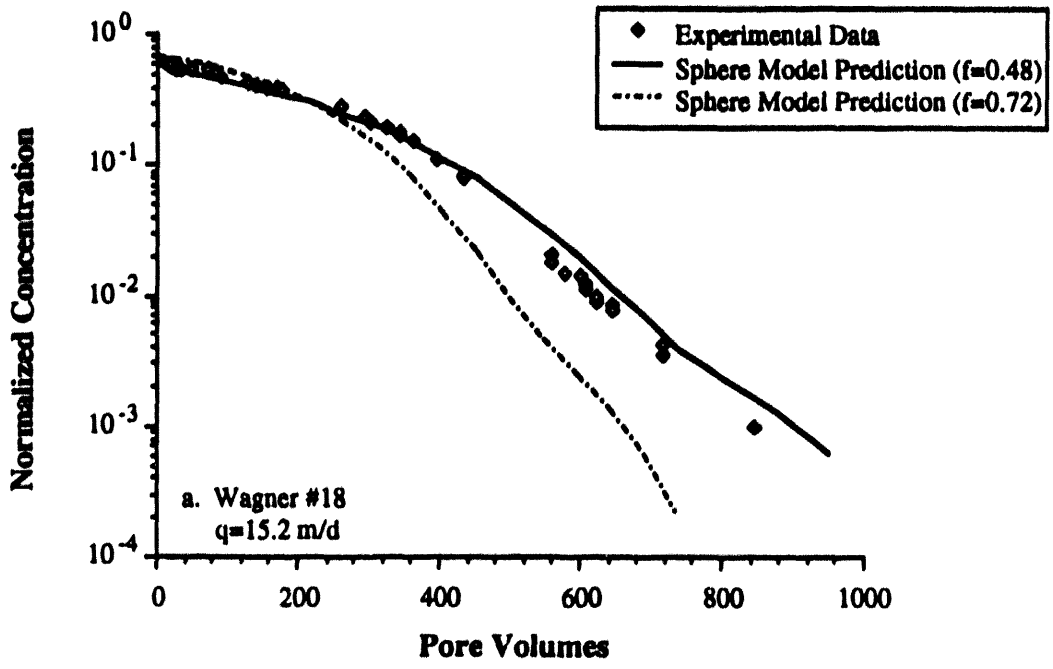

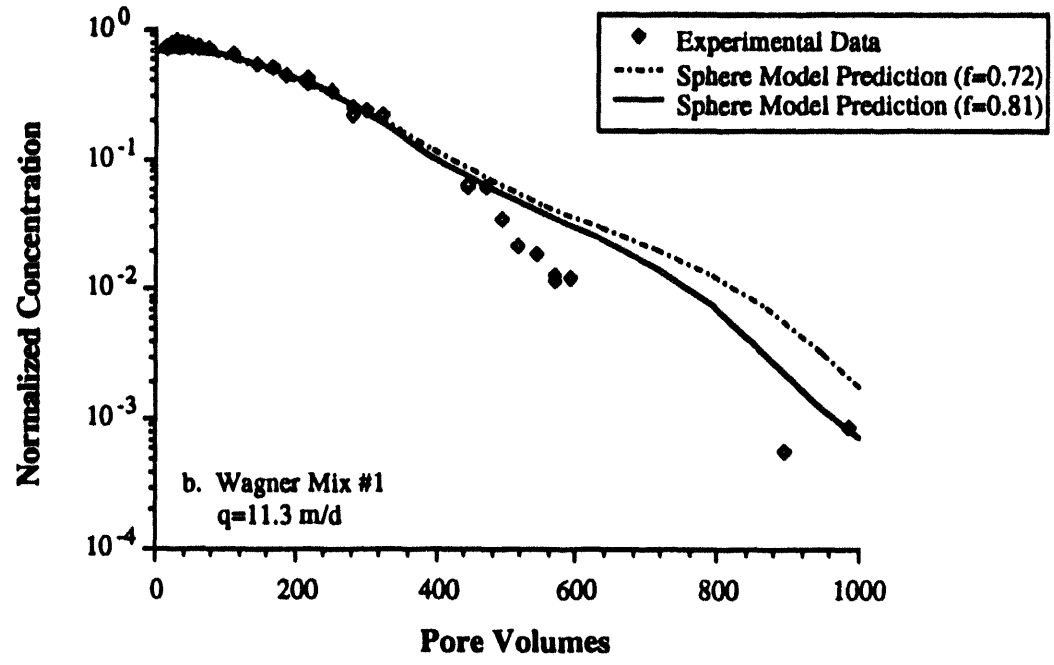

Figure 4.3.7: Prediction of Transient TCE Dissolution Data with Sphere Model: a. Uniform Sand; and b. Graded Sand

Comparison of model predictions to experimental data is illustrated in Figures 4.3.7a and b. The model was an excellent predictor of TCE dissolution from Wagner #18 sand (Figure 4.3.7a). Prediction of effluent concentrations from experiments utilizing graded sand were not as good (Figure 4.3.7b). The sphere model did not adequately reproduce the location of changes in slope of the data as plotted in the figures. The significance of this is hard to determine due to the lack of data points at very low (<1 mg/l) concentrations. In all cases, sphere model predictions based on average f_m values for each sand were superior to those based on the overall average f_m value (f_m=0.72). Further discussion of the sphere model can be found in Powers *et al.* (1993b).

Alternative Transient Dissolution Models

Miller *et al.* (1990) developed a correlation for the modified Sherwood number in terms of the Reynolds number and volumetric fraction of NAPL in the system. The range of NAPL volumetric fractions considered was based on the amount of NAPL stirred into a packed bed of glass beds. This correlation:

$$Sh' = 425(\varepsilon-\theta^n)\, Re'^{0.75}\, \theta^{n\ 0.60} \qquad (4.3.6)$$

was determined from a series of steady state dissolution experiments.

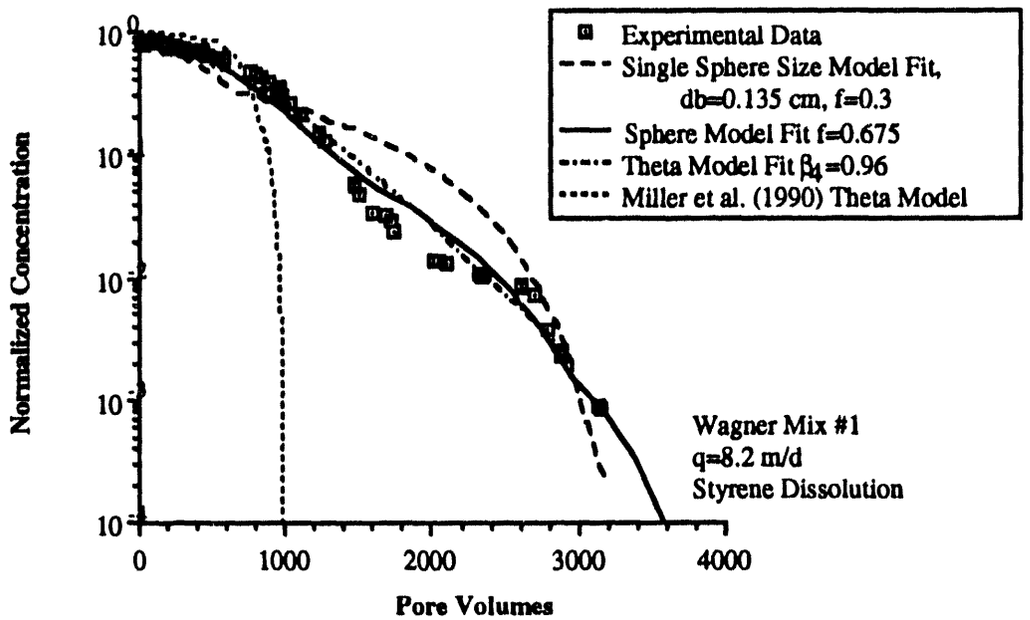

Figure 4.3.8: Comparison of Model Simulations

A simpler version of the sphere model described above has been used by Geller (1990) to describe effluent concentrations of benzene from column experiments. Benzene was entrapped in the middle portion only of a glass bead pack, resulting in flow of water through and around the NAPL contaminated region. Geller utilized a mass transfer coefficient correlation developed for a packed bed of naphthalene spheres (Wilson and Geankoplis, 1966), and assumed that NAPL blobs were distributed as mono-sized spheres with all of the surface area exposed to mobile water (f_m=1.0); the initial diameter of NAPL spheres was used as a fitting parameter. Geller found that, simulations from this model, with initial sphere diameters ranging from 0.15-0.40 cm, closely matched experimental data.

Figure 4.3.8 compares simulations from the two models described above with predictions of the sphere and theta models developed in this work. The simulations considered styrene dissolution in a graded sand. The figure indicates that the Miller *et al.* correlation significantly underpredicts the volume of water required to remove styrene from the sand examined. The single-size sphere model of Geller does a better job of reproducing the data, but shows significantly more curvature than suggested by the data.

5.0 TWO DIMENSIONAL MODELING

The sphere model described above was incorporated into a two-dimensional numerical simulator in order to predict and investigate NAPL dissolution processes in field scale settings, as described in Abriola *et al.* (1993).

The simulator was used in conjunction with a multiphase flow simulator to explore the transport and fate of a spill of TCE occurring in a layered system of fine sands. The simulators were used to examine the potential influence of soil heterogeneities, both in controlling the initial formation of the NAPL residual saturation distribution, and in the long term dissolution and flushing of the residuals. Prediction of field scale dissolution processes can also be substantially affected by non-equilibrium mass transfer limitations. Mass transfer coefficients used in this work were established from laboratory measured steady-state napthalene dissolution experiments performed by Dunkin (1991) (eq. 4.2.7).

The simulation scenario presented in Figure (5.1) involves a lower permeability layer located between two higher permeability strata. Permeabilities in the two formations differ by a factor of two. A spill of TCE occurs for a period of 15 days, after which redistribution of the NAPL and dissolution occurs. An impermeable boundary is located at the base of the domain, with hydrostatic conditions imposed at the left and right boundaries.

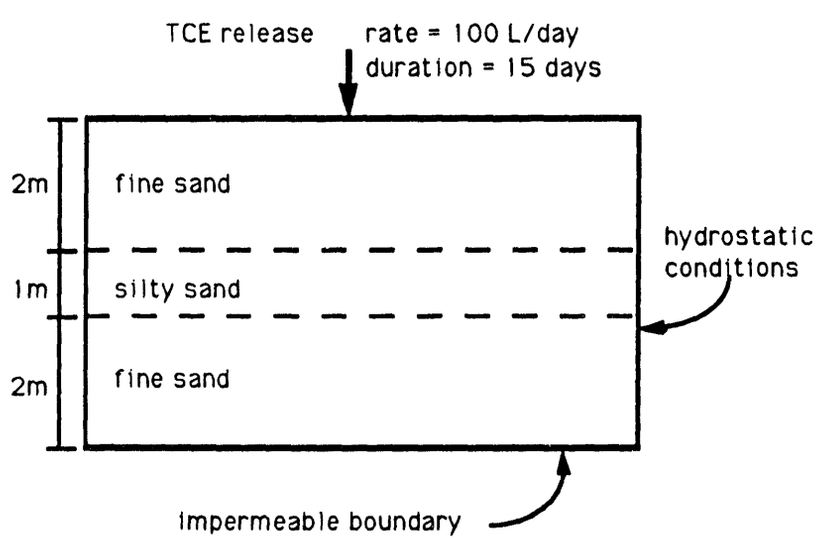

Figure 5.1 Configuration of the simulation domain

The initial NAPL distribution and, consequently, the methodology used to predict the distribution are critical to the prediction of the overall removal efficiencies. Here a "realistic" residual distribution of TCE was established by employing predictions from a multiphase flow simulator which accounts for hysteretic entrapment processes (Abriola *et al.*, 1992). Simulation of the NAPL spill and subsequent dissolution was carried out sequentially. Coupled flow equations describing the simultaneous migration of water and TCE were solved initially, assuming an absence of NAPL dissolution. This assumption is reasonable given the relatively fast migration of the NAPL, low solubility of the TCE and the large quantities of water which must be flushed past the organic in order to fully remediate the site. After a quasi-residual TCE distribution was established, a regional water gradient was imposed through the domain to induce dissolution.

Results of a migration/dissolution simulation are presented in Figure (5.2) for the duration of the contamination event. The upper two plots present the predicted TCE saturations from the multiphase flow model. The effects of the lower permeability stratum are clearly evident in the first plot. The downward vertical migration of the NAPL is impeded by this layer, causing ponding and lateral spreading. After building up sufficient pressure head for breakthrough, some of the NAPL continues on a downward course until the lower impermeable boundary is encountered. After one year of redistribution, the TCE was assumed to be effectively immobile.

Following emplacement of the NAPL residual, the two-dimensional dissolution simulator was used to simulate long-term dissolution of the TCE residuals under a regional groundwater gradient of 0.005 m/m. The steady-state mass transfer correlation developed by Dunkin (1991) was used in conjunction with the sphere model presented above to predict rates of mass transfer between the organic and aqueous phases. TCE residual blobs were modeled as uniform spheres, with an initial diameter estimated from correlation of the mean grain size of entrapped styrene blobs as reported in Powers (1992). At each time step the saturation dependent relative permeability of water was evaluated using a scaled vanGenuchten (1980) form for relative

permeability. A summary of all input parameters used in the simulator may be found in Abriola *et al.* (1993).

The bottom four plots of Figure (5.2) show the progression of TCE dissolution and flushing as a result of the regional groundwater flow. As expected, TCE removal is observed to occur primarily on the upstream (left) side of the zone of entrapment, where the concentration driving force (eqn 2.1.1) is the greatest. The effects of heterogeneity are also clear. Permeability and, consequently, flow rates are largest in the upper and bottom layers. This results in greater rates of dissolution and flushing in these layers, even though the majority of TCE mass is entrapped in these layers. Overall flushing time is prolonged by the lower flow rates encountered in the middle layer.

The simulation performed illustrates the influence of soil heterogeneities, both in controlling the formation of the initial NAPL distribution and in the rate of NAPL dissolution. NAPL drainage in a layered system, with a permeability difference of one-half, was substantially impeded by the soil stratum, causing significant lateral spreading in the upper layer. In the simulation of NAPL dissolution and flushing, an overall reduction in the flushing rate was observed due to bypassing and lower flow rates in the less permeable layer. Ultimately, simulations reveal that accurate representation of field scale dissolution processes is substantially influenced by three phenomena: the residual NAPL distribution, the rate of NAPL interphase mass transfer, and soil heterogeneities.

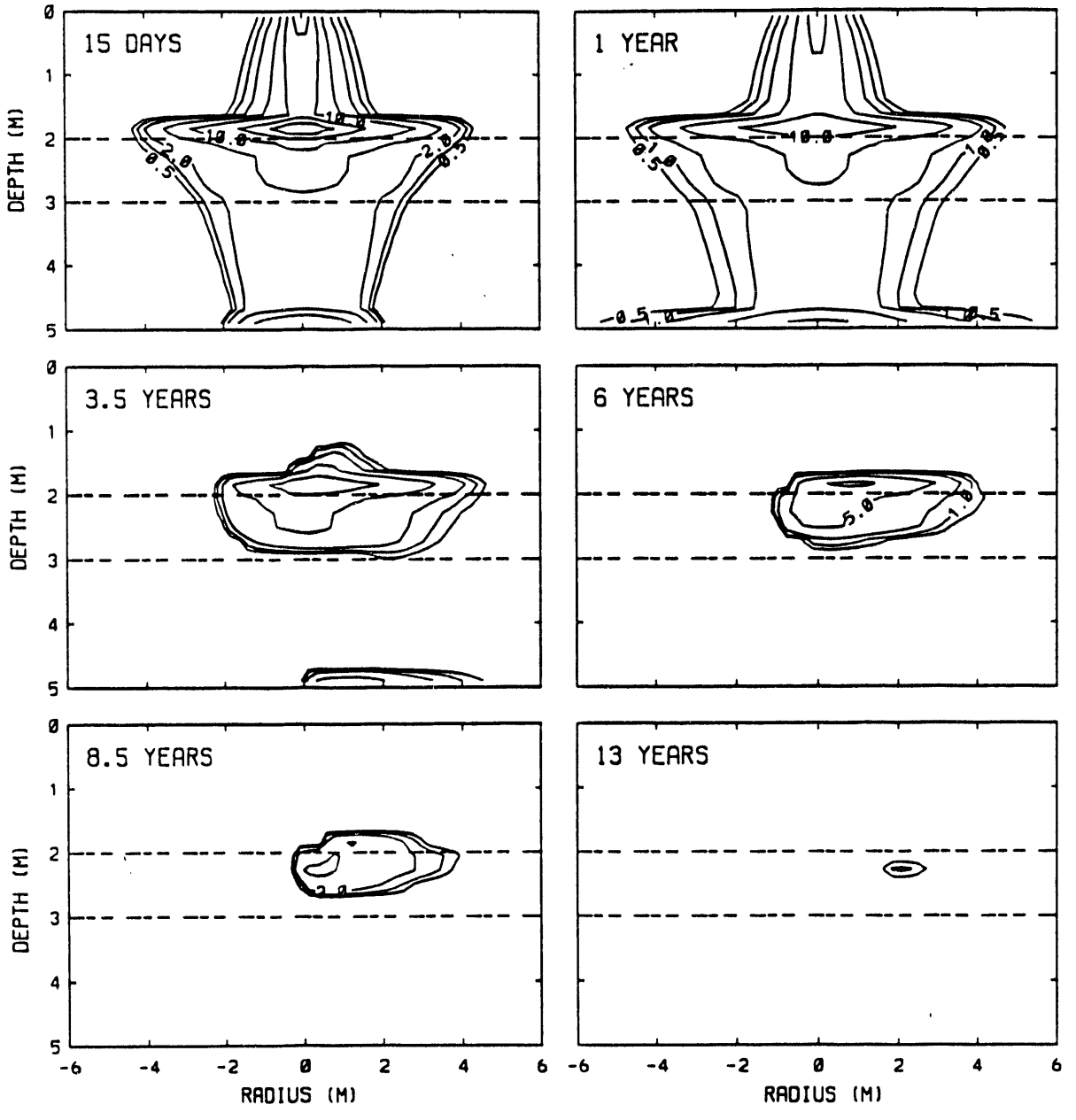

5.2 Predicted TCE saturation distributions. Contour intervals are: 0.5, 1.0, 2.0, 5.0, 10.0, 20.0, and 30.0 percent TCE saturation.

6.0 CONCLUSIONS AND RECOMMENDATIONS

6.1 Conclusions

The presence of nonaqueous phase liquids in the subsurface creates a long-term source of pollution which is difficult to remedy. A general lack of understanding of the physical and chemical phenomena governing the fate of these contaminants limits our ability to develop effective remediation strategies to reduce public health risk associated with these spill sites. The focus of this research work was on the development of a better understanding of the NAPL-water interphase mass transfer processes. Broadly stated, the objectives of this work were the experimental measurement of NAPL dissolution rates in laboratory sand columns, the development of phenomenological models for these rates in terms of measurable soil and fluid properties, and the application of these models to evaluate the potential significance of non-equilibrium processes. The primary hypotheses of this research were that: 1) the local equilibrium assumption may not adequately describe dissolution rates under high aqueous phase flow rates; 2) the distribution of NAPL in the subsurface is a crucial parameter impacting mass transfer processes; and, 3) these NAPL distributions, and hence dissolution rates, are a function of the pore structure of a porous medium.

Several specific conclusions were reached based on the experimental results of this work.

- NAPL blob distributions depend on porous medium properties. Entrapped blobs were larger in coarse sands than in fine sands because the pore bodies are larger in the coarse media. In graded media, small-scale heterogeneities led to the entrapment of a few, large (~0.5-cm diameter) NAPL blobs.

- Effluent concentrations from one-dimensional column experiments varied with aqueous phase velocity. Greater deviations from equilibrium conditions occur at high aqueous phase velocities due to the reduction in contact time between phases.

- Steady-state effluent concentrations also varied with porous medium characteristics. Differences in the volumetric fraction of NAPL entrapped in the columns did not account for these discrepancies. More styrene was entrapped in the Wagner Mix #1 sand than in the medium-fine Wagner #50 sand, but, effluent concentrations from the column packed with the graded sand were lower.

- Results of transient dissolution experiments indicate that deviations from equilibrium are greater in coarse and graded sands. More than twice as much water was required to reduce effluent concentrations from the coarse Wagner #18 to 1% of the equilibrium concentration than required for the finer Wagner #50 sand.

- NAPL shape and size distributions can beused to explain the dependence of dissolution rate on porous medium characteristics. The larger blobs entrapped in

coarse and graded sands have less specific surface area across which mass transfer can occur resulting in slower dissolution rates in comparison with dissolution rates in finer, uniform media.

- Due to decreasing interfacial area for mass transfer as entrapped organic is dissolved, mass transfer limitations under transient conditions were found to be more significant than in the steady-state case.

These conclusions support the original hypotheses of this work. It was demonstrated that there are conditions under which the local equilibrium condition cannot adequately describe NAPL dissolution in laboratory-scale columns. Furthermore, it was shown that dissolution rates are very sensitive to porous medium properties, due to differences in blob shape and size distributions.

Specific conclusions reached based on the mathematical modeling of dissolution processes include:

- In correlations for the modified Sherwood number, the inclusion of parameters quantifying pore-structure properties as surrogate measures of surface area greatly improved the phenomenological models' capacity to describe variation in steady-state dissolution rate data (high R^2 values).

- Based on the results of the model verification, it is concluded that the optimal steady-state mass transfer rate model is the correlation for the modified Sherwood number in terms of the Reynolds number and grain-size-distribution parameters:

$$Sh' = 8.41\ Re^{0.61}\ \delta^{0.64}\ U_i^{0.41}$$

- Phenomenological models for long-term dissolution of NAPLs must account for the decreasing surface area as NAPL mass is removed from the system. The relationship between decreasing surface area and time depends on blob shape and, hence, porous medium characteristics.

- Both the theta and sphere models developed in this work can fit transient styrene dissolution data for a range of sands. An assessment of the quality of the fit, as quantified with the sum-of-square difference between model simulations and experimental data, indicates that the theta model fits data from coarse or graded sands better than the data from medium to fine uniform sands.

- The calibration parameter for the theta model, β_4, is correlated to grain-size-distribution properties.

- The calibration parameter for the sphere model, f_m, varies among sand types, but is not statistically correlated to grain-size parameters or aqueous phase velocities.

- The sphere model is conceptually more appealing than the theta model. However, this model requires a substantial amount of input data to describe blob distributions. The theta model only requires gain-size-distribution parameters and a good estimate of the initial residual saturation, making it easier to implement than the sphere model.

- Due to the incorporation of parameters describing the differences in pore structure among different types of sand, there is less error between transient dissolution data

and model simulations for those developed in this work than for those in recent literature. Thus, it may be feasible to apply the theta model to NAPL dissolution problems in sandy media, other than those tested herein. Other models in the literature, however, have limited potential for application.

The laboratory- derived phenomenological models for interphase mass transfer were incorporated into a two-dimensional transport simulator. This simulator should be a useful tool for the analysis of the impact of mass transfer limitations at a larger scale. This numerical modeling work indicated that:

- Nonequilibrium processes may have a pronounced effect on field-scale dissolution processes.
- Soil heterogeneities play a significant role in field scale NAPL dissolution, both in controlling the formation of the initial NAPL distribution and by affecting the rate of NAPL dissolution.

6.2 Recommendations for Further Research

The primary focus of continued research efforts in this area should be to understand and quantify the impact of heterogeneity on NAPL dissolution processes. Both field-scale and pore-scale heterogeneities could substantially impact NAPL dissolution rates and, hence, could adversely affect engineering approaches to remedying NAPL spill sites. An improved understanding of NAPL-water mass transfer processes could provide insight into a wide range of remedial alternatives, including bioremediation and enhanced pump-and-treat methods. Specifically, future research in the area of NAPL dissolution should include:

- Exploration of alternative means for assessing pore-scale NAPL blob distributions and subsequent scaling to field scale systems.
- Experimental investigation of the relationship between scale, NAPL distribution and dissolution rates in larger column, sand box and field-scale experiments.
- Investigation of the distribution of NAPL and subsequent dissolution rates in heterogeneous porous media.
- Development of a methodology to scale results from NAPL dissolution laboratory column experiments to larger scale systems.
- Further development of numerical models to assess implications of rate-limited NAPL dissolution processes.
- Measurement of mass transfer rates in other aquifer remedial alternatives.

REFERENCES

Abriola, L.M. and G.F. Pinder. 1985a. A Multiphase Approach to the Modeling of Porous Media Contamination by Organic Compounds: (1) Equation Development. *Water Resour.Res.* 21(1): 11-18.

Abriola, L.M. and G.F. Pinder. 1985b. A Multiphase Approach to the Modeling of Porous Media Contaminated by Organic Compounds: (2) Model Development. *Water Resour.Res.* 21(1): 19-26.

Abriola, L.M. 1989. Modeling Multiphase Migration of Organic Chemicals in Groundwater Systems: A Review and Assessment. *Environmental Health Perspectives* 83:117-143.

Abriola, L.M., T.J. Dekker, and K.D. Pennell, "Surfactant Enhanced Solubilization of residual dodecane in soil columns. 2. Mathematical Modeling", ES& T, in press.

Abriola, L.M., T.J. Dekker, and K.M. Rathfeller, 1993, "Recent advances in the modeling of organic liquid contaminant migration and persistence in aquifer systems" presented at the second USA/CIS Joint Conference of Environmental Hydrology and Hydrogeology

Abriola, L.M., K. Rathfelder, S. Yadav, and M. Maiza, 1992, "VALOR: a PC Code for Simulating Surface Immiscible Contaminant Transport", Final Report, Electric Power Research Institutue, Palo Alto, Ca.

Baehr, A.L. 1987. Selective Transport of Hydrocarbons in the Unsaturated Zone Due to Aqueous and Vapor Phase Partitioning. *Water Resour.Res.* 23(10): 1926-1938.

Bear, J. *Dynamics of Fluids in Porous Media*, Elsevier, New York:1972.

Bordon, R.C. and C.M. Kao. 1989. Water Flushing of Trapped Residual Hydrocarbons, Mathematical Model Development and Laboratory Validation. In: *Proceedings - Petroleum Hydrocarbons and Organic Chemicals in Groundwater: Prevention, Detection and Restoration*, p. 473-486. Worthington, Ohio: National Water Well Association.

Brooks, R.H. and A.T.Corey. 1966. Properties of Porous Media Affecting Fluid Flow. *Journal of Irrigation and Drainage Division of ASCE* 92(IR2):61-68.

Boundy, R.H., R.F. Boyer and S.M. Stoesser. 1965. *Styrene: Its Polymers, Copolymers and Derivatives, Part I.* New York: Hafner Publishing Company.

Chatzis, I., N.R.Morrow and H.T.Lim. 1983. Magnitude and Detailed Structure of Residual Oil Saturation. *Soc.Pet.Eng.J.* 311-326.

Cherry, J.A., S.Feenstra, , B.H.Kueper, and D.W.McWhorter, Status of In-Situ Technologies for Cleanup of Aquifers Contaminated by DNAPLs Below the Water Table. In: *presented at the International Specialty Conference on How Clean is Clean? Cleanup Crieria for Contaminated Soil and Groundwater (Air and Waste Management Association; November 6-9)*, Washington,D.C.: 1990,

Conrad, S.H., J.L. Wilson, W.R. Mason and W.J. Peplinski. 1992. Visualization of Residual Organic Liquid Trapped in Aquifers. *Water Resour.Res.* 28(2):467-478.

Corapcioglu, M.Y. and A.L. Baehr. 1987. A Compositional Multiphase Model for Groundwater Contamination by Petroleum Products: (1) Theoretical Considerations. *Water Resour.Res.* 23(1): 191-200.

Dean, J.A. (ed.). 1973. *Lange's Handbook of Chemistry*, 11th edition. New York: McGraw-Hill.

deMarsily, G. 1986. *Quantitative Hydrology: Groundwater Hydrology for Engineers.* Orlando: Academic Press.

deZabala, E.F. and C.J. Radke. 1986. A Non-Equilibrium Description of Alkaline Water Flooding. *Soc.Pet.Eng.J.* 26(1): 29-43.

DOE, Subsurface Science Program: Program Overview and Research Abstracts, FY1989-1990, 1991.

Dorgarten, H.W. and C.F. Tsang. 1990. Three-Phase Simulation of Organic Contaminants in Aquifer Systems. Presented at the *Conference on Subsurface Contamination by Immiscible Fluids (International Association of Hydrology; April 18-20)*. Calgary, Alberta.

Driscoll, F.G. 1986. *Groundwater and Wells, 2nd edition*. St.Paul, MN: Johnson Filtration Systems.

Dullien, F.A.L. *Porous Media: Fluid Transport and Pore Structure* , New York:Academic Press, 1979.

Dunkin, J.S. 1991. Measurement of Naphthalene Sphere Dissolution Rates. Report # EWRE-91-001. Ann Arbor, MI: The University of Michigan, Department of Civil Engineering.

Feenstra, S. and J. Coburn. 1986. Subsurface Contamination from Spills of Denser than Water Chlorinated Solvents. *California WPCF Bull.* 23(4): 26-34.

Fried, J.J., P. Muntzer and L. Zilliox. 1979. Groundwater Pollution by Transfer of Oil Hydrocarbons. *Ground Water.* 17(6): 586-594.

Geller, J.T. and Hunt, J.R., 1993 Mass transfer from Nonaqueous Phase Organic Liquids in Water-Saturated POrous Media. Water Resour. Res., 29:833-846.

Geller, J.T. Dissolution of Non-Aqueous Phase Organic Liquids in Porous Media, PhD Dissertation, University of California . In: , Berkley,CA: 1990,

Guarnaccia, J.F., P.T. Imhoff, B.C. Missildine, M. Oostrom, M.A. Celia, J.H. Dane, P.R. Jaffe and G.F. Pinder. 1992. Multiphase Chemical Transport in Porous Media. EPA Environmental Research Brief, EPA/600/S-92/002. Ada, Oklahoma: Robert S. Kerr Environmental Research Laboratory.

Holusha, J. 1991. When Water Isn't The Only Thing Coming Out Of The Well. *The New York Times*

Hunt, J.R., N. Sitar and K.S. Udell. 1988. Non Aqueous Phase Liquid Transport and Cleanup: (2) Experimental Studies. *Water Resour.Res.* 24(8): 1259-1269.

Imhoff, P.T., P.R. Jaffe, and G.F. Pinder. 1990. Dissolution of Organic Liquids in Groundwater. In: *Proceedings of the American Society of Civil Engineers, 1990 Specialty Conference*, p. 290-298. Arlington,VA.

Keely, J.F., Performance Evaluations of Pump-and-Treat Remediations, USEPA Office of Research and Development- Office of Solid Waste and Emergency Response, EPA/540/4-89-005, 1989.

Kueper, B.H., E.O.Frind, and D.B.McWhorter, The Behavior of Dense Nonaqueous Phase Liquid Contaminants in Heterogeneous Porous Media . In: *Contaminant Transport in Groundwater*, edited by Kobus, H.E. and W.Kinzelbach, Rotterdam: Balkema Publishers, 1989,

Kumar, S., S.N. Upadhyay and V.K. Mathur. 1977. Low Reynolds Number Mass Transfer in Packed Beds of Cylindrical Particles. *Ind.Eng.Chem.Process Des.Dev.* 16(1): 1-8.

Larson, R.G., H.T.Davis and L.E.Scriven. 1981. Displacement of Residual Nonwetting Fluid from Porous Media. *Chem.Engng.Sci.* 36:75-85.

Li, Y. and N.C.Wardlaw. 1986. The Influence of Nonwettability and Critical Pore-Throat Size Ratio on Snap-Off. *J.Colloid Interface Sci.* 109(2):

Mackay, D.M., P.V.Roberts and J.A.Cherry. 1985. Transport of Organic Contaminants in Ground Water. *Environ.Sci.Technol.* 19(5):384-392.

Mercer, J.W. and R.M.Cohen. 1990. A Review of Immiscible Fluids in the Subsurface: Properties, Models, Characterization and Remediation. *J.Contam.Hydrol.* 6: 107-163.

Miller, C.T., M.M.Poirier-McNeill and A.S.Mayer. 1990. Dissolution of Trapped Nonaqueous Phase Liquids: Mass Transfer Characteristics. *Water Resour.Res.* 26(11):2783-2796.

Miller, C.T., M.M. Poirrer-McNeill and A.S. Mayer. 1990. Dissolution of Trapped Nonaqueous Phase Liquids: Mass Transfer Characteristics. *Water Resources Research* 26(11):2783-2796.

Mohanty, K.K., H.T.Davis and L.E.Scriven. 1987. Physics of Oil Entrapment in Water Wet Rocks. *SPE Reservoir Engineering* 2:113-127.

Morrow, N.R. and C.C.Harris. 1965. Capillary Equilibrium in Porous Materials. *Soc.Pet.Eng.J.* 5:15-24.

Morrow, N.R. and I.Chatzis, Measurement and Correlation of Conditions for Entrapment and Mobilization of Residual Oil, Report, DOE/BETC/3251-12. In: , 1981,

Morrow, N.R. 1970. Irreducible Wetting-Phase Saturations in Porous Media. *Chem.Engng.Sci.* 25:1799-1815.

Morrow, N.R. 1970. Physics and Thermodynamics of Capillary Action in Porous Media. *Industrial and Engineering Chemistry* 62(6):32-56.

Morrow, N.R. 1971. Small-Scale Packing Heterogeneities in Porous Sedimentary Rock. *Bull.Assoc.Petrol.Geol.* 55(3):514-522

Ng, K.M., H.T.Davis and L.E.Scriven. 1978. Visualization of Blob Mechanism in Flow Through Porous Media. *Chem.Engng.Sci.* 33:1009-1017.

Parker, J.C., A.K. Katyal, J.J. Kaluarachchi, *et al.* 1990. Modeling Multiphase Organic Chemical Transport in Soils and Groundwater. Final Report, U.S. EPA-Project #CR-814320.

Perry, R.H. and C.H. Chilton. 1973. *Chemical Engineers Handbook, 5th Edition*. New York: McGraw-Hill.

Pfannkuch, H.-O. Determination of the Contaminant Source Strength from Mass Exchange Processes at the Petroleum-Groundwater Interface in Shallow Aquifer Systems. In: *NWWA Conference on Petroleum Hydrocarbons and Organic Chemicals in Ground Water*, 1984,

Powers, S.E., C.O.Loureiro, L.M.Abriola and W.J.Weber. 1991. Theoretical Study of the Significance of Nonequilibrium Dissolution of Nonaqueous Phase Liquids in Subsurface Systems. *Water Resour.Res.* 27(4):463-477.

Powers, S.E., L.M. Abriola, and W.J. Weber, Jr. 1992, "An experimental investigation of Nonaqueous Phase liquid dissolution in saturated subsurface systems: Steady state mass tranfer rates", *Water Resour.Res.* 28(10):2691-2705.

Powers, S.E., L.M. Abriola, and W.J. Weber, Jr, "An experimental investigation of NAPL dissolution in satuated subsurface systems: Transient Mass Transfer Rates", submitted to *Water Resour.Res.*, Feb. 1993

Powers, S.E., L.M. Abriola, J.S. Dunkin, and W.J. Weber, "Phenomenological Modles for Transient NAPL-Water Mass Transfer Processes" submitted to J. Contamin. Hydrol. 1993.

Razakarisoa, O., J.D. Rasolofoniaina, P. Muntzer, and L. Zilliox. 1989. Selective Dissolution and Transport of Hydrocarbons in an Alluvial Aquifer- Role and Impact of Residual Air on Ground Water Contamination. In: *Contaminant Transport in Grou. Jwater*, edited by H.E.Kobus and W. Kinzelbach. Rotterdam: Balkema Press.

Schiegg, H.O. 1980. Field Infiltration as a Method for the Disposal of Oil-in-Water Emulsions from the Restoration of Oil-Polluted Aquifers. *Water Resour.Res.* 14(6):1011-1016.

Schwille, F. Dense Chlorinated Solvents in Porous and Fractured Media, Translated by J.F. Pankow. In: , Chelsea, MI: Lewis Publishers, 1988,

Sleep, B.E. and J.F.Sykes. 1990. The Influence of Infiltrating Wetting Fronts on Transport of Volatile Organic Compounds in Variably Saturated Porous Media. Presented at the *Conference on Subsurface Contamination by Immiscible Fluids (International Association of Hydrology; April 18-20)*. Calgary, Alberta.

Testa, S.M. and D.L.Winegardner, Restoration of Petroleum Contaminated Aquifers. In: , Chelsea, MI: Lewis Publishers, 1991,

Tsakiroglu, C.D. and A.C. Payatakes. 1990. A New Simulator of Mercury Porosimetry for the Characterization of Porous Materials. *J.Colloid Interface Sci.* 137(2):315-339.

van Genuchten, M.T. 1980. A Closed Form Equation for Predicting the Hydraulic Conductivity of Unsaturated Soils. *Soil Sci.Soc.Amer.J.* 44: 892-898.

Vershueren, K. 1983. *Handbook of Environmental Data on Organic Chemicals*. New York: Van Nostrand Reinhold.

Voss, C.I. A Finite-Element Simulation Model for Saturated-Unsaturated, Fluid-Density-Dependent Ground-Water Flow with Energy Transport or Chemically-Reactive Single Species Solute Transport, U.S. Geological Survey. In: , Reston, VA: 1984,

Wardlaw, N.C. 1982. The Effects of Geometry, Wettability, Viscosity and Interfacial Tension on Trapping in Single Pore-Throat Pairs. *J.Can.Petrol.Tech.* 21(3):21-27.

Weast, R.C. and M.J. Astle (eds). 1981. *CRC Handbook of Chemistry and Physics*, 62nd edition. Boca Raton, Florida: CRC Press.

Weber, W.J. *Physicochemical Processes for Water Quality Control*, New York:John Wiley and Sons, 1972.

Weber, W.J. and E.H.Smith. 1991. Simulation and Design Models for Adsorption Processes. *Environ.Sci.Technol.* 21(11):1040.

Weber, W.J., P.M.McGinley and L.E.Katz. 1991. Sorption Phenomena in Subsurface Systems: Concepts, Models, and Effects on Contaminant Fate and Transport. *Water Res.* (In Press)

Welty, J.R., C.E.Wicks, and R.E.Wilson, *Fundamentals of Momentum, Heat and Mass Transfer*, New York:John Wiley, 1969.

Wilke, C.R. and P.Chang. 1955. Correlation of Diffusion Coefficients in Dilute Solutions. *AIChE J.* 1(2):264-270.

Wilson, J.L., S.H.Conrad, W.R.Mason, W.Peplinski, and E.Hagan, Laboratory Investigations of Residual Liquid Organics from Spills, Leaks and Disposal of Hazardous Wastes in Groundwater, Final Report, U.S. EPA-EPA/600/6-90/004. In: , 1990

Wilson, E.J. and C.J. Geankoplis. 1966. Liquid Mass Transfer at Very Low Reynolds Numbers. *Ind.Eng.Chem.Fund.* 5(1): 9-14.

Wray, K.W. 1986. *Measuring Engineering Properties of Soils*. Englewood Cliffs, NJ: Prentice Hall, Inc.

Published Work and Presentations

Powers, S. E., L. M. Abriola, and W. J. Weber, Jr., "The Effect of Interphase Mass Transfer Rates on the Extent of Aquifer Contamination by NAPLs," presented at the *ACS 22nd Central Regional Meeting*, Saginaw, MI, June 1990.

Abriola, L. M., "Modeling Non-aqueous Phase Liquid Migration and Persistence in the Unsaturated Zone - Progress and Perspective," presented at *Characterization of Transport Phenomena in the Vadose Zone*, a Workshop sponsored by SSSA and AGU, Tucson, AZ, April 1991. (invited paper)

Powers, S. E., L. M. Abriola, J. S. Dunkin, and W. J. Weber, Jr., "Experimental Assessment of the Impact of Pore Structure on Interphase Mass Transfer Rates and Blob Distributions During NAPL Dissolution Processes," *AGU Symposium on Recent Advances in the Understanding of Nonideal Interphase Transport in Porous Media*, Baltimore, MD, May 1991. (invited paper)

Dunkin, J.S. 1991. Measurement of Naphthalene Sphere Dissolution Rates. Report # EWRE-91-001. Ann Arbor, MI: The University of Michigan, Department of Civil Engineering.

Powers, S.E., L. M. Abriola, and W.J. Weber, Jr., "Experimental Assessment of Factors Limiting Transient NAPL-Water Mass Transfer Processes," *AGU Spring Meeting*, Montreal, May 1992.

Powers, S.E., L. M. Abriola, and W.J. Weber, Jr., "Development of Phenomenological Models for NAPL Dissolution Processes," Extended abstract, *Proceedings of the Subsurface Restoration Conference 3rd International Conference on Groundwater Quality Research*, Dallas, TX, June 1992.

Abriola, L.M., S.E. Powers, and W.J. Weber, Jr., "Investigation of the Dissolution of Nonaqueous Phase Organic Liquid Contaminants in Soils," Proceedings of the NATO-ASI Conference on *Migration and Fate of Pollutants in Soils and Subsoils*, Maratea, Italy, May-June, 1992.

Abriola, L.M., T.J. Dekker, S.E. Powers, and K.D. Pennell, "Implications of rate-limited NAPL-water mass transfer processes on two-dimensional field scale remediation efforts," *Soil Science Society of America 84th Annual Meeting*, Minneapolis, MN, November 1992.

Powers, S.E., L. M. Abriola, and W.J. Weber, Jr., "A Phenomenological Model for Transient NAPL Dissolution Processes," *AGU Fall Meeting*, San Francisco, CA, Dec 1992.

Powers, Susan E., Linda M. Abriola, and Walter J. Weber, Jr., "An Experimental Investigation of NAPL Dissolution in Saturated Subsurface Systems: Steady-State Mass Transfer Rates," *Water Resources Research*, 28 (10), 2691-2705, 1992.

Abriola, Linda M., Timothy J. Dekker, and Klaus M. Rathfelder, "Recent Advances in the Modeling of Organic Liquid Contaminant Migration and Persistance in Aquifer Systems," *Proceedings Second USA/CIS Joint Conference on Enviromental Hydrology and Hydrogeology*, May 10-12, 303-316, Washington, DC, 1993.

Powers, Susan E., Linda M. Abriola, Joyce S. Dunkin, and Walter J. Weber, Jr., "Phenomenological Models for Transient NAPL-Water Mass Transfer Processes," submitted to *Journal of Contaminant Hydrology*, 1993.

Powers, Susan E., Linda M. Abriola, and Walter J. Weber, Jr., "An Experimental Investigation of NAPL Dissolution in Saturated Subsurface Systems: Transient Mass Transfer Rates," submitted to *Water Resources Research*, 1993.

DATE
FILMED
1/12/94

END